Geo 511
Master's Thesis

Spatio-temporal quantification of geomorphological processes in the recently deglaciated area surrounding the Findelengletscher

Alexander Ruff
Matr.-Nr.: 05-052-535

supervised by:
Prof. Dr. Andreas Vieli, faculty member (3G)
Dr. Isabelle Gärtner-Roehr (3G)

Glaciology and Geomorphodynamics Group - 3G
Department of Geography, University of Zurich
Winterthurerstrasse 190
CH-8057 Zürich

Submitted 30/1/2015

Abstract

The ongoing melting of the Findelengletscher in the Swiss Alps exposes landscapes that are in an unstable or metastable state, and consequently accountable to modification, erosion, and sediment release. These areas are highly dynamic regarding sediment transfer by different processes. Typically glacial, gravitational, periglacial, and glacio-fluvial processes occur in close proximity and on different temporal scales. The purpose of this study is to identify and map the morphodynamics in the paraglacial environment and monitor the temporal evolution of the found processes. Thereafter the sediment transfer rates of the found processes are quantified.

Based on a unique dataset of high-resolution DSMs (1m) from multi-temporal LiDAR campaigns (2005, 2009, 2010) and an additional survey in 2014 using a drone eBee the landforms and the corresponding morphodynamics are mapped. The annual elevation loss for the whole study site (without the glacier) is -240 mma^{-1} and exceeds denudation rates by two magnitudes. Responsible for the sacking is the melt of ice-cored moraines, dead-ice blocks, and debris covered parts of the glacier. The modification of sediment-mantled slopes shows that reworking lateral moraines which started with the deglaciation have slowed down to a rate of -250 mma^{-1} due to the beginning exhaustion of sediments. Glacio-fluvial erosion rates diverge considerably depending on the spatio-temporal settings. The uncertainties assessment shows that the error is at least one magnitude smaller than the elevation changes and offers reliable results.

Acknowledgments

First of all, I would like to express my gratitude to my supervisors, Prof. Dr. Andreas Vieli and Dr. Isabelle Gärtner-Roehr, without whom this master thesis would not have been possible. I would like to thank them for their support, patience and always granting me access to their office and giving me advice and encouragement.

Dr. Philip Claudio Jörg was ever so helpful and introduced and led me through the whole work concerning the acquisition of the 2014 dataset. Processing the data and helping me out with my gaps in remote sensing would not have been manageable without him.

Further I would like to thank Larissa, Lea, Eve and Martin for proofreading my thesis.

Very special thanks are owned to my colleagues working with me in 'G10'. Their support when having a motivation crisis, a GIS problem, a formating issue in LaTeX, or just having a coffee break helped me finishing this thesis.

My academic studies at the University of Zürich would not have been possible without the support of my parents. Thank you for your generosity, patience and support throughout all these years.

Last but not least I would like to thank my girlfriend for her encouragement in stressed times.

Contents

List of Figures

List of Tables

List of Abbreveations

DSM	Digital Surface Model
DTM	Digital Terrain Model
GIS	Georaphic Information System
GPR	Ground Penetrating Radar
GPS	Global Positioning System
LCS	Local Contrast Stretch
LiDAR	Light Detection and Ranging
RRS	Residual Relief Separation
first period	2005 - 2009
second period	2009 - 2010
third period	2010 - 2014

List of Definitions

geomorphometry	processing DEM (Hengl & Reuter 2009)
gradient	measures the steepness of slope (rate of change of elevation) (Otto & Smith 2013)
morphometry	Is the science of quantitative land-surface analysis (Pike et al. 2009)
paraglacial	nonglacial earth-surface processes, sediment accumulations, landforms, landsystems and landscapes that are directly conditioned by glaciation and deglaciation (Ballantyne 2002*b*)

1 Introduction

1.1 Motivation

In most mountain areas glaciers are retreating due to the global warming e.g. (Paul et al. 2008). In the European Alps the volume of the glaciers was diminished by 50% in the last 150 years (Haeberli & Beniston 1998) and therefore drastically changed the geomorphology in these areas. The sediment sources stripped through deglaciation are in an unstable or metastable state and are vulnerable to processes of release, reworking and redeposition at rates greatly exceeding denudation rates (Curry et al. 2006). Remodification rates for processes in the paraglacial period are known, but the precise changes of a part of the period have not been explored yet.

The availability of a repeated high resolution Light Detection and Ranging (LiDAR) dataset provides a unique opportunity for quantifying different geomorphological processes acting in the recently deglaciated area with a high temporal and spatial resolution. Such images are expensive to obtain and were used to quantify the volume of the glacier. The data was exclusively used to investigate processes of the glacier. In this thesis however, the glaciated area will be ignored and everything surrounding it is going to be used. The goal of this master's thesis is therefore to make use of the unique dataset and not only map and describe the observed processes, but also to quantify them.

1.2 Research on Findelengletscher

Lot of research has been conducted on Findelengletscher in the past decade thanks to the following reasons (Joerg et al. 2012): its easy accessible with the Air Zermatt and benefits of the excellent infrastructure of the ski resort of Zermatt. The glacier surface is nearly debris free and has a fairly constant slope, which enables in situ measurements of almost every part of the glacier. In addition the glacier is expected to last multiple decades of strong melt because of its size and ranging from 2600 m a.s.l. to 3900 m a.s.l.

The list of research done is long and reaches back over thirty years. Here are some selected research topics that have been amongst others addressed in the past years: Glaciological research (Iken & Bindschadler 1986), longterm in situ measurements being conducted by the Universities of Fribourg and Zürich e.g.(Büchel 2011), snow accumulation distribution measurements from helicopter-borne ground penetrating radar (GPR) (Machguth et al. 2006, Sold et al. 2013), volumetric changes from digital surface models (DSM) (Kääb 2005, Joerg et al. 2012, Joerg & Zemp 2014, Bossard 2014), runoff modeling and runoff projections (Uhlmann et al. 2013, Huss et al. 2014) as well as studies concerning the foreland and moraines (Lukas et al. 2012, Madella 2013).

1.3 Objectives

The objectives of this master's thesis are thus the following:

- Expand the time series with drone flights over the study site from five to nine years.
- Create a geomorphologic map showing the morphodynamics.
- Distinguish stable areas from areas that are in movement (erosion and deposition).
- Find out which processes are active and where.
- Quantify the sediment transfer budget for the active zones.

2 State of the art

2.1 Pararglacial concept

Deglaciation in mountain areas expose large surfaces of unstable or metastable sediment sources. They are vulnerable to processes of release, reworking and redeposition at rates greatly exceeding denudation rates (Curry et al. 2006). These geomorphological activities are named *paraglacial* and were introduced by Church & Ryder (1972). (Ballantyne 2002*b*, 1938) gives the following definition for *paraglacial*: "nonglacial earth-surface processes, sediment accumulations, landforms, landsystems and landscapes that are directly conditioned by glaciation and deglaciation" and defines the *paraglacial period* as "a period of readjustment from a glacial to a nonglacial condition"(Ballantyne 2002*b*, 1937). The term paraglacial is similar to the term proglacial but not quite the same. *Proglacial* is defined by geologists and "describes the location on which a suite of processes is operative, whereas paraglacial implies that particular processes have in some way been conditioned by glaciation, and would operate at different rates (or not at all) had glaciation not occurred" Ballantyne (2002*b*, 1993). There are six paraglacial landsystems: rockslopes, drift-mantled slopes, glacier forelands, and alluvial, lacustrine and coastal systems. Elements of these paraglacial landsystems relax at different rates. Ballantyne (2002*b*, 1937) gives the example that "steep, sediment-mantled hillslopes (...) may achieve stability within a few centuries of ice retreat, whereas large fluvial systems may still be reworking glaciogenic sediment more than 10'000 years after deglaciation". The paraglacial period therefore varies in different landscape context and also in spatial scale.

2.1.1 Paraglacial modification of sediment-mantled slopes

The retreat of the glacier reveals steep slopes mantled by thick unvegetated glacigenic deposits, usually composed of stacked lateral moraines. Such deposits resting against the slope at steep gradients are susceptible to erosion by slope failure, debris flow, snow avalanches, tributary streams and surface wash (Ballantyne 2002*b*). Under these conditions lots of volume of lateral moraine can be transported, forming a paraglacial landsys-

tem of valley-side gullies, slope-foot debris cones and valley-floor deposits.

2.1.2 Processes

The main cause for erosion and sediment transport occurring on steep sediment-mantled slopes is debris flow (sediment-gravity flow), a quick downslope flow of poorly sorted sediment and water (Ballantyne 2002*b*). Debris flow on steep drift-mantled slopes exposed by the retreat of valley glaciers have been observed in the Canadian Rockies, in the Karakoram (Owen 1994), in the Swiss Alps (Zimmermann & Haeberli 1993, Rickenmann & Zimmermann 1993) as well as in Norway (Ballantyne & Benn 1994). Some flows are initiated by rainstorms, whereas others happen during the spring melting of snow in the gully heads (Ballantyne & Benn 1994). Debris flows are the dominant agent of erosion on steep sediment mantled slopes. There is evidence that lateral moraines are also reworked by fluvial action, surface wash, rainsplash, snow and slush avalanches, and aeolian deflation (Curry et al. 2006).

In some occasions part of the moraine may collapse (e.g. Tasman Glacier in New Zealand (Blair 1994) or the Findelengletscher). Ice-cored lateral moraines are especially prone to rapid failure, because the melting of the ice inside reduces the strength of the overlying sediment (Sigurdsson & Williams 1991, Richardson & Reynolds 2000).

The gully systems cut deep into the tall lateral moraines, and the debris cones are accumulated downslope as shown in Figure 2.1. Not all recently deglaciated drift-mantled slopes receive extensive paraglacial modification (Ballantyne 2002*b*). The driving factors controlling the extent of sediment transfer are the gradient of slope of the moraine, the relief, and the moisture availability (Curry et al. 2006).

Landforms

Gullies are separated by sharp 'arêtes' of sediment. bottom reworked debris, usually appearing in the form of coalescing debris cones (Curry 2000, Ballantyne 2002*b*).

2.1.3 Rates of activity

Curry et al. (2006) show that paraglacial activity correlates with the gully index (see Table 2.1) and average moraine gradient. For the Swiss Alps there seems to be a threshold gradient exceeding ca. 30° representing a prerequisite for extensive paraglacial modification of sediment-mantled slopes. There also appears to be a limit that the moraines have to be at least 120 m high. Landscapes fulfilling these two preconditions do not necessarily imply that extensive gullying actually occurs. There must be other important factors

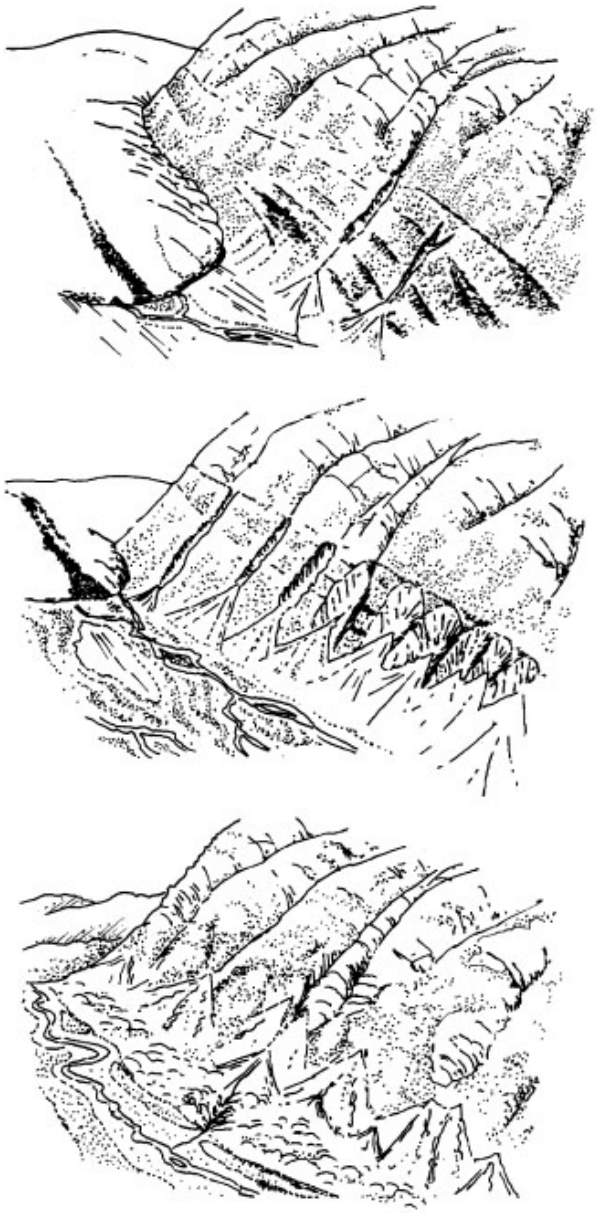

Figure 2.1: Landforms associated with three stages in the paraglacial reworking of drift-mantled slopes. Top: Initial slopes exposed by glacier retreat, showing lateral moraines and the onset of gully incision. Middle: Advanced gully development and the deposition of coalescing debris cones. Bottom: Exposed bedrock and stabilized, vegetated gully systems at the head of relict debris cones. By this final stage, paraglacial sediment reworking has effectively terminated due to exhaustion of sediment supply from upslope sites (Ballantyne 2002*b*).

that Curry et al. (2006) left out (e.g. the presence of buried ice, moraine sedimentology and geotechnical properties), a likely autocorrelation of independent variables that control the modification of moraine slopes.

The activity ends when the gully system stabilizes as a result of sediment exhaustion. At the Swiss sites of Feegletscher and Glacier du Mont Miné the "primary glacigenic sediment stores have been depleted, whereas reworked sediment has accumulated as slope-foot landforms or experienced secondary transfer by fluvial processes" (Curry et al. 2006, 224).

Average rates have been calculated over the whole period from deglaciation until nowadays and are compared to other sites in Norway where the rates are smaller (see Table 2.2). An attempt to determine short-term rates of net surface lowering was attempted on Feegletscher (Curry et al. 2006). From September 2000 to September 2002 50 pins were installed at a depth of 2 m along the slope-foot debris sheet. However, only seven of the pins were re-measured. The rest of the pins were buried or removed by debris flow activity. The authors explain (Curry et al. 2006, 221): "Whilst the limitations of data collected over such a brief time period must be emphasized, these values do help to provide an indication of the magnitude of slope adjustment and the range of internal variation at a single site". The rate of net sedimentation for erosion was 4-48 $\mathrm{mm}\,a^{-1}$ (Curry et al. 2006).

Attempts to calculate short term erosion by using DSMs as tried in this thesis have not been done so far. This is most likely due to the nonexistence of such expensive high resolution datasets of three different years.

2.2 Denudation rates in the Alps

Denudation is a surface process that leads to the removal of material from the Earth's surface, and generally leads to a lowering of the surface. The study area is affected by such processes.

Hinderer et al. (2013) calculated an area-weighted average of the total denudation rate of 0.32 $\mathrm{mm}\,a^{-1}$ for the Alps and 0.42 $\mathrm{mm}\,a^{-1}$ for pre-dam areas. The rates are higher when looking at the Alps in the paraglacial cycle after deglaciation in the Late Glacial (17-11.6 ka BP) and post-glacial. It is 0.62 $\mathrm{mm}\,a^{-1}$ for the entire Alps in the post-glacial and 1.76 $\mathrm{mm}\,a^{-1}$ in the Late Glacial. In the Turtmanntal, a valley west of the study site, the denudation rates range between 0.62-1.87 $\mathrm{mm}\,a^{-1}$ and 1.42-2.64 $\mathrm{mm}\,a^{-1}$ for the Hungertälli, a small sub-valley where the uncertainties are much smaller than for the entire valley. However, there is no valley glacier there as the one of the study site.

	Gullying index[a]	Average slope gradient	Maximum slope height (m)	Average elevation of crest (m)	Slope aspect	Topographic setting[b]
Val d'Hérens and vicinity						
1. Gl. de Tsijiore Nouve	2	30°	50	2300	150°	1
2. Bas Glacier d'Arolla	3	31°	150	2150	050–075°	2
3. Glacier du Mont Miné	3	32°	180	2050	065–095°	2
4. Glacier de Ferpècle	3	31°	180	2100	320–010°	2
5. Glacier de Bricola	2	34°	60	2800	120°	1
Saaser valley and vicinity						
6. Zmuttgletscher	3	34°	140	2450	150–170°	2
7. Gornergletscher	2	34°	120	2500	345–025°	3
8. Findelgletscher	3	34°	120	2550	160–205°	3
9. Bidergletscher	1	32°	50	2250	180–190°	1
10. Hohbalmgletscher	2	33°	60	2550	205°	1
11. Feegletscher North (N)	3	36°	120	2000	165–240°	3
12. Feegletscher North (S)	1	22°	80	2125	330–010°	3
13. Feegletscher South	1	29°	50	2225	130–150°	1
14. Hohlaubgletscher	2	33°	60	2500	160–190°	1
15. Allalingletscher	2	34°	80	2450	155–175°	1
16. Triftgletscher	2	34°	60	2700	150–175°	1
17. Mälligagletscher	1	25°	20	2950	175°	1

[a] 1: <10 gullies per kilometre; 2: 10–40 gullies per kilometre; 3: >40 gullies per kilometre.
[b] 1: valley-floor; 2: valley-side; 3: combination.

Table 2.1: Site characteristics and extent of paraglacial gully erosion on the proximal slopes of recently deglaciated lateral moraines at Findelengletscher, and at other nearby sites (Curry et al. 2006).

Location	Rate (mm yr^{-1})			Timescale (yr)	Source
	Min.	Mean	Max.		
Gully incision					
Glacier du Mont Miné T_1[a]	86	107	151	<55	Curry(2006)
Feegletscher T_1[a]	49	75	103	<79	Curry(2006)
Bergsetbreen, Jostedalen	37	—	94	<215	Ballantyne (1995)
Fåbergstølsbreen, Jostedalen	50	72	100	<49	Ballantyne and Benn (1994)
Fåbergstølsbreen, Jostedalen	38	94	169	<53	Curry (1999)
Lodalsbreen, Jostedalen	19	92	169	<43	Curry (1999)
Heillstugubreen, Jotunheimen	5.5	7.7	8.8	<76	Curry (1999)
Søre Illåbreen, Jotunheimen	2.5	2.8	3.0	<247	Curry (1999)
Langtang Himal, Nepal	0.4	3.4	8.0	<550	Watanabe *et al.* (1998)
Cone accumulation					
Glacier du Mont Miné	—	31	—	<142	Curry(2006)
Bergsetbreen, Jostedalen	8	—	44	<215	Ballantyne (1995)
San Rafael Glacier, Patagonia[b]	330	—	400	<16	Harrison and Winchester (1997)

[a] T_{2-4} survey data has been excluded, owing to the highly degraded nature of these gully systems.
[b] Timing of the onset of debris accumulation is derived from lichenometric dating of cone surfaces, thus these values are likely to be over-estimates.

Table 2.2: Rates of gully incision and debris cone accumulation on recently deglaciated terrain. (Curry et al. (2006) modified).

2.3 Lateral Moraines

Research concerning Alpine lateral moraines can be roughly put into three themes according to Lukas et al. (2012):

- Reconstructing former, mostly lateglacial, glacier extents using morphostratigraphic principles
- numerical dating of glacier fluctuations
- establishing genetic processes of moraine formation (Small 1983)

The modification as well as erosion of lateral moraines are not mentioned. In the paraglacial context these topics are addressed. However, there is no reference linking the two fields of study.

2.4 Geomorphological Mapping

By definition of Gustavsson et al. (2006), a geomorphological map should contain information on morphometry, morphography, hydrography, lithology, structure, age, and process/genesis. It is a challenging task to pack all the information into one single map. That is why "..geomorphological maps have become a result of a number of choices, related to the extent and history of the area, the mapping scale and the geomorphological characteristics given highest priority, e.g. presented in color in the map"(Gustavsson et al. 2006, 92).

2.5 Geomorphological legends

There have been several attempts to uniform the geomorphological legends in the past years.

Gustavsson et al. (2006, 91): "Geological maps, which are generally more simple in their structure than geomorphological maps, have to some extent succeeded in keeping their legends uniform, but geomorphological maps have not: either local conditions emphasize presentation of specific features at the cost of others, or the legends are so exhaustive that they reduce readability."

The geomorphological parameters morphometry, morphography, hydrography, lithology, structure, age, and process/genesis and the use of visual variables (Bertin 1983) offer numerous possibilities of combination (Gustavsson & Kolstrup 2009). In the following sections some selected legend systems are introduced.

The GIUZ legend

All the recent master theses written at the Department of Geography of the University of Zürich (GIUZ) use the same legend key. They are mainly used in highmountain regions of the Engadin at a scale of 1:25'000 and cover all process domains. However there was no publication to be found introducing the key to the scientific world. Each process domain uses its own color and forms are displayed mostly in similar colors or with textures. The example legend (Figure 2.2) shows only features and processes that are being used. However the legend is compatible with all process domains.

Figure 2.2: An example of the GIUZ legend (Zuan 2008).

The IGUL legend

The geomorphological mapping legend of the University of Lausanne (IGUL) has been used for over 20 years in high and middle mountain regions (Maillard et al. 2009). The bundle can be used as an ArcGIS extension. It offers a geodatabase which already has got the three feature datasets for point, line and area features. Colors represent the process categories. The signatures use the same color of the related process and have a genetic significance (see Figure 2.3). The morphodynamics differentiation of erosion and accumulation areas is made visible by white and colored surfaces. However morphography, slopes and lithology are not represented in the legend key.

The legend of Jan-Christoph Otto

Jan-Christoph Otto offers a geomorphologic legend key for highmountains (see Figure 2.4) that can be downloaded from his website http://www.geomorphology.at/ and be integrated into the ArcGIS environment. Predefined colors for the processes can be imported and the signatures are imported as new font which has to be installed in the operating system. It is made for maps with a scale of 1:25'000 and is based on the legendsystem for highmountains from Kneisel et al. (1998), who adapted the GMK25 (Barsch & Liedtke 1980).

The legend of Gustavsson

Gustavssons legend combines symbols for hydrography, morphometry/morphography, lithology and structure with color variations for process/genesis and geologic age (see Figure 2.5). Therefore it is designed for many different types of geomorphologic maps and all of them can rely on the same simple legend key.

Every legend system has got their advantage. Some of them are optimized for a specific area whilst others hold general settings which should work under all circumstances but not always be the best solution. For this thesis an new legend system is developed using whichever suits the requirements best.

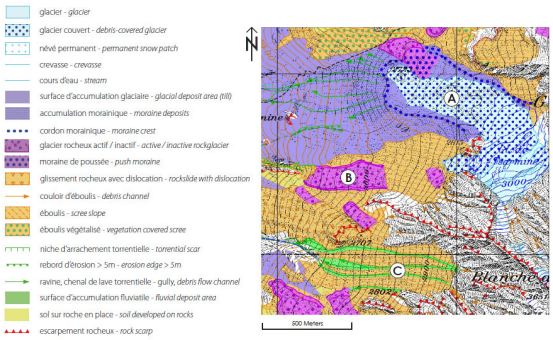

Figure 2.3: Example of the geomorphological mapping legend of the University of Lausanne, used on the Tsarmine area, Arolla valley (VS) (Lambiel et al. 2013).

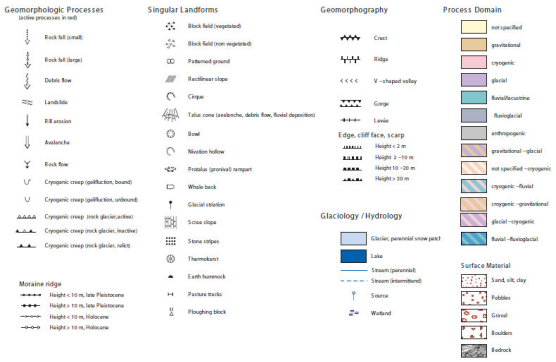

Figure 2.4: Example legend of the geomorphological map in the Turtmanntal (VS) (Otto & Dikau 2004).

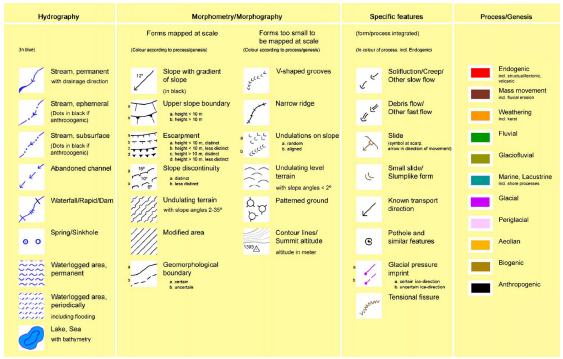

Figure 2.5: Legend developed by Gustavsson et al. (2006). The categories lithology, structure, and age are not shown since they will not be used in the map created in this thesis.

3 Study site and data

This thesis is based on a unique dataset of four high resolution DSMs. Furthermore, the following products from the Federal Office of Topography swisstopo are used.

3.1 Study site

The study site is the paraglacial area of the Findelengletscher (also called Findelgletscher), which is located in the area of Zermatt, in the south-eastern part of the Swiss Alps (46°00'N, 7°49'E). The Findelengletscher is one of the largest temperate valley glaciers in the Alps (Maisch et al. 2000), ranging from about 2600 m a.s.l. to 3900 m a.s.l. and consisting of Findelengletscher and its former tributary Adlergletscher which was separated from the Findelengletscher in the 1990s so that they form two independent glaciers now (Joerg et al. 2012). In 1850 (last glacial maximum) the Findelengletscher had a length of 10.4 km (Maisch et al. 2000). Since then the glacier retreated to a length of 7.8 km in 1973 (Maisch et al. 2000) and to 6.7 km in 2010 (Joerg et al. 2012) revealing a large glacial foreland formerly covered by ice. The foreland is escorted by two prominent lateral moraines as can be seen in Figure 3.1. The lateral moraines stand up to 140 m above the valley floor, are over 3 km long and strongly asymmetrical in cross-profile. The distal slopes range from 29° to 36° and the proximal slopes from 41° to 64°, but locally reach angles of up to 80°.

The study site is limited to the area that all measurements have got in common (see *red* area in Figure 3.1). The bottom limit is about where the moraine of 1991 defines the natural border leading all the run-off to the gauging station (Madella 2013). The left and right side borders are the lateral moraines, including the steep sloped area on the right side where the slide broke through the moraine (see Figure A.7).

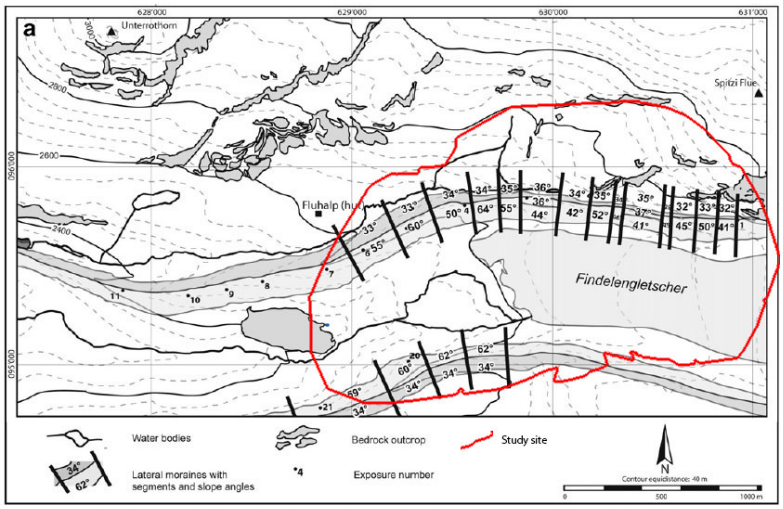

Figure 3.1: Overview of slope angles of the lateral moraines at Findelengletscher combined with the precise study site. The outline of the study site is shown in *red* (Lukas et al. (2012) modified).

3.2 Data

3.2.1 LiDAR

The three DSMs are derived from airborne laser scanning taken on the 28. and 29.10.2005, the 4.10.2009, and the 29.09.2010 with a resolution of 1 m (Joerg et al. (2012), Joerg & Zemp (2014) for detailed information). The DSM covers the whole Findelen- and Adlergletscher and their surroundings. The uncertainties for single raster cells on the glacier are less than 0.10 m and more for the non glaciated area. That is because small shifts have got a larger height error in steeper terrain than on the flat glacier. In 2005, 13 days prior to the measurement there was heavy snowfall in the region, depositing 65 cm of snow on Gornergrat. In the days after the snowfall a lot of snow melted away. Thanks to the meteostation based on Gornergrat, the snowmelt was modeled for the whole altitude range of the study site and taken into consideration when calculating the DSM. In the lower elevation of this study site, some snow was left on the glacier, however the glacier forefield should have been almost snowfree (personal information from Philip Jörg). 2009 was complete snow free and is therefore the most precise dataset of these three.

Glacier outlines

The glacier outlines from the Findelen- and Adlergletscher are derived from the LiDAR data of the years 2005 to 2010 and aerial images (Glacier Laserscanning Experiment Oberwallis, (GLAXPO-project)). The 2014 outline is digitized out of the DSM and from the orthophoto of the same year.

3.2.2 Federal Office of Topography swisstopo

The Federal Office of Topography swisstopo offers a large variety of products. The following ones are used in this thesis.

swissALTI^{3D}

SwissALTI^{3D} is the most precise digital terrain model (DTM) product from the Federal Office of Topography swisstopo, describing the surface of Switzerland without vegetation or development (version used: 2013). Above 2000 m above sea level the average error is 1 - 3 m.

SWISSIMAGE

The orthophoto mosaic of Switzerland SWISSIMAGE is arranged out of digital aerial photographs. The newest images date from 2012 and have got a resolution of 50 cm.

Swiss Raster Map 25

The Swiss Raster Map 25 (SRM 25) is the digital version of the 1:25'000 printed map that is for sale in all stores (version used: 15.02.2010). The map is world wide well-known for its high detail content and accuracy in mountainous regions.

swissTLM^{3D}

swissTLM^{3D} shows man-made and natural features in vector format with height information, that can be directly used in a geographic information system (GIS). Of the eight thematic layers hydrography, buildings, roads and tracks, and rock areas out of the land cover layer are used (version used: 1.2).

3.2.3 Dataset 2014

The measurements of 2014 were taken by flying a drone over the study site. A powerful software comes along with the drone and produces an orthophoto and a DSM of the overflown area.

eBee the drone

eBee is a fully autonomous mini-drone from the École Polytechnique Fédérale de Lausanne (EPFL) spinoff senseFly. The fixed-wing aircraft carries position and altitude sensors along with a camera and a communication unit. The software is intuitive and lets you plan, simulate, monitor, and control the trajectory of the eBee both before and during the flight. Depending on the wanted accuracy the parameters such as flight height, percentage of overlapping, and resolution can be defined. Experienced users can set up a flight campaign in about 10 minutes.

4 Methods

4.1 Workflow

The schema shows in chronological order the steps taken to create the geomorphological map. Each step is described either in the following sections or in another chapter. Cross references indicate the location of sections outside of this chapter.

1. Viewing of the 2005, 2009, and 2010 datasets (see subsection 3.2.1)
2. Definition of study area (see section 3.1)
3. Conceptual outline of the map
4. Geodatabase design, structure and process domains
5. Geodatabase implementation
6. Fieldwork 2014 and data collection (see section 5.1)
7. Redefining the study area because of 2014 data
8. Digitizing and morphometry
9. Map visualization and legend generation
10. Quantification of processes

4.2 Conceptual outline of the map

The aim of the map is to visualize the ongoing processes in the paraglacial environment of the Findelengletscher in the year 2014 together with morphodynamics that can be found there. Out of the whole dataset the year 2014 is chosen because of several reasons. First, there exists an aerial image of the same time as the DSM. Besides all the morphometric information that can be generated out of the DSM (see section 4.5), the colored aerial image can give additional inputs. Second, after generating a first version of the map,

ground proof can be found of the exact same situation and not of an older situation. The map is mainly intended to be the starting point to look at spatial and temporal aspects to evaluate if they are continuous or episodic, and to quantify them. There has been much research done on the Findelengletscher. But is there in no existing geomorphological map available. This map intends to close the gap and provide the scientists with easily accessible information that may support their research studies. The map will be optimized for printing and has a large scale of 1:7000. The extent of the map is on one hand given through the extent of the data and on the other hand by the area of interest focusing on the paraglacial environment. Information concerning the processes, some specific forms, hydrology, and morphometry are displayed. However, classifications of lithology, structure and age (except moraines) are left out, because the map would get too crowded and these informations are least important to answer the research questions.

4.3 Geomorphological process domains

Process domains are defined as regions within which one or a collection of earth surface processes prevail for the detachment and transport of mass (Brardinoni & Hassan 2006). The mass movements are all facing downwards due to gravitation but that does not classify all areas in the gravitational process domain. Only the dominant one or a mix of the two dominant ones are selected. Distinguishing them from one and another and defining them is difficult and represents the main problem when generating the geodatabase design and creating the legend concept. Depending on whose book or article one reads, the list of geomorphological processes are mostly the same with small wording differences (e.g. periglacial or cryogenic) (Leser 2003). Only those process domains and forms are presented that are being displayed on the map.

Gravitational process domain

All processes are influenced by gravitation. They are mostly supported by other forces or processes such as fluvial or glacial ones. Areas that are mapped in the gravitational process domain are those where gravitation predominately triggers the mass movements.

Glacial process domain

Processes and landforms assigned to the glacial process domain are shaped by glaciers and their motions. Looking at the whole study site, nearly everything is in some way influenced or formed by the glacier. However, as the glacier retreats, other processes

overlap and reform the landscape. There are only small regions left after the reformation that are in the glacial process domain, as most of them are combined. The ground moraine and the three small hills in the outwash plain are the sole glacial forms on the map. The prominent lateral moraines all have partially glacial process domains and will be described in the according subsection.

Periglacial process domain

The area of the periglacial process domain lies often near a glacier and depends on ice and frost related processes. Periglacial areas are to be found where temperatures are low and are closely related to the extent of permafrost. The two rockglaciers found above the right lateral moraine as well as the slide collapsing the moraine are forms in the periglacial process domain.

Fluvial process domain

The fluvial process domain includes areas that are primarily created by running water. The processes are vary seasonally and can be triggered by one event (e.g. precipitation, outburst of a lake).

Gravitational-glacial process domain

The gravitational-glacial process domain covers areas where both gravitational and glacial processes are dominant. The biggest parts of the lateral moraine where only small movements are taking place are assigned to that domain.

Glacial-periglacial processes domain

In the other parts of the lateral moraine a much bigger mass movement can be found. This creeping mass movement has a higher watercontent than in the other areas.

Glacio-fluvial process domain

In the study areas fluvial processes are mostly linked to glacial ones as the sediment is produced by the glacier and is transported and deposited by fluvial processes. Below the glacier there are three deep eroded channels through the ground moraine guiding the alluvium to the outwash plain where most of it is being deposited.

4.4 Geodatabase desing and implementation

In the past decade several Master theses of the University of Zurich had the aim of creating a geomorphological map e.g. (Zuan 2008, Felber 2011, Brun 2012). The newer ones refer to the older ones and not to published literature. In this thesis a look on my predecessors' work is allowed but the emphasis is on published articles. Therefore the work flow of this map as well as the visual appearance will be somewhat different. The geomorphological maps of the before mentioned theses 2008, 2011, and 2012 were looking at whole valleys on smaller scales whereas this map is drawn at a scale of 1:7000. So there will be smaller forms and areas to distinguish from each other in this theses as well as different or big branches of processes which are not found in the area of interest.

4.4.1 Geodatabase design

The geodatabase design scheme that is used to construct the geodatabase is the one proposed by Gustavsson et al. (2008), however all use similar layer systems e.g.(Haeberling 2000):

1. geomorphological feature dataset
2. hydrographical feature dataset
3. geological feature dataset
4. other feature classes and non-spatial tables inside the geodatabase
5. additional data connected to the geodatabase

All classes but the geological feature dataset are used in this map. The geomorphological forms and processes are mapped with points, lines, and polygons. The following topology rules are implemented in order to have a consistent and logical geodatabase (Demel & Hauenstein 2005):

- Polygons must not have gaps.
- Polygons must not overlap.
- Points must be disjoint.

consequently:

- Lines may overlap lines or polygons.
- Points may overlap lines or polygons.

If processes are overlapping or could not be identified clearly, the decision has to be made which is the dominant form or process.

4.4.2 Geodatabase implementation

The geodatabase is created similar to the ones in the theses of Koch (2003), Beer (2005), Imbaumgarten (2005), Zuan (2008), Felber (2011) and the one of Gustavsson et al. (2008).

When digitizing an areal object in ArcGIS an ID ("OBJECTID*") and geometry properties ("SHAPE*", "SHAPE_Length", "SHAPE_Area") are saved in the attribute table (Figure 4.1). The "OBJECTID*" gives each entry a unique value. "SHAPE*" defines if the object is a point, line or polygon, "SHAPE_Length" and "SHAPE_Area" show the size of the object. Geomorphologic attribute fields are added to specify the objects as follows: "D_ID" for dynamic properties , "M_ID" for material properties, "P_ID" for process properties, "Y_ID" for the year the object presents, and "SHAPE_ID" which can contain a comment or name of the form or process. Each field can be filled by selecting an attribute from the predefined drop-down window. This design helps to query the geodatabase, e.g. to find all erosive objects that have a glacial process domain.

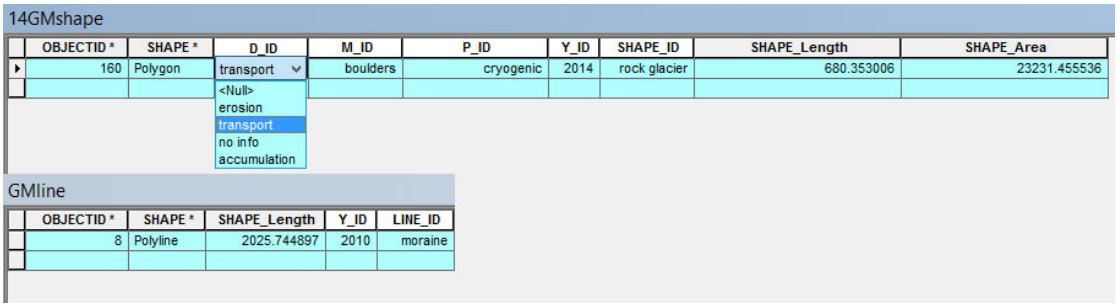

Figure 4.1: Tables of line and polygon objects. In the dynamic properties field, the drop-down selection can be seen. Drop-down fields are also available for the material properties and the process properties.

Linear and point objects have similar fields. The ones ArcGIS generates are the same as for a polygon except that the "SHAPE_Area" is missing for linear objects and the "SHAPE_Area" and "SHAPE_Length" is missing for point objects. The self defined attributes are again "Y_ID" and "LINE_ID" which define the type of line or "POINT_ID" for points in comparison to the "SHAPE_ID" for areas.

Alternatively the existing geodatabase of the University of Lausanne could have been used. The effort of creating the geodatabase would have been much easier, however there are some aspects the database of Lausanne cannot handle. Every form is classified to a specific signature. Querying for all signatures in the glacial process domain that show erosion is not possible. One would have to select all signatures manually. This is a big disadvantage whenever the focus is not only on the creation of the map but also on using the data to see other features that cannot easily be seen in the original map.

4.5 Geomorphometry

According to Smith & Wise (2007) the results of mapping glacial landforms depend on two factors:

- *Landform detectability.* The degree to which the physical and spectral characteristics of the sensor allows the landforms to be distinguished form other features on the image.
- *Observer ability.* The success with which an observer can record these differences and thus map the landforms.

They describe three main controls on landform representation:

(1) *relative size.* The size of the landform relative to the spatial resolution.

(2) *azimuth biasing.* The orientation of the landform with respect to solar azimuth.

(3) *landform signal strength.* The tonal/textural differentiation of the landform.

4.5.1 Visualization techniques

There are different visualization techniques available that help with interpreting a DSM. The interpretation of these images is a demanding task for the sense of vision and requires a lot of concentration (Demel & Hauenstein 2005). Despite all different techniques, the interpretation of these images always depends on the skill and experience of the user. That is why ground truth must be sought to check out the made interpretations.

Relief shading

Relief shading or hillshade is an effective method to identify landforms on a DSM (Smith & Wise 2007). However one has to be careful because adding an artificial illumination may lead to azimuth biasing. Depending on the direction and the angle of the illumination, features may be easier to detect or remain unseen. Multiple (best orthogonal) illumination directions are recommended for optimal detection (Smith & Clark 2005), and a solar elevation angle of $<20^\circ$ helps to increase the visual features through shadowing (Smith & Wise 2007).

Gradient and curvature

Gradient is an often used method to measure the steepness of slopes. Curvature shows the rate of change of gradient. Three commonly used curvatures related to the gravity field are described by Schmidt et al. (2003): profile curvature, planform curvature (often also called contour curvature) and tangential curvature.

Profile curvature is parallel to the slope and is good to identify breaks of slope (Figure 4.2). Plan curvature is perpendicular to the slope and highlights gullies and ridges in flow direction (Figure 4.3). Curvature perpendicular to slope gradient is called tangential curvature but was not used in this thesis.

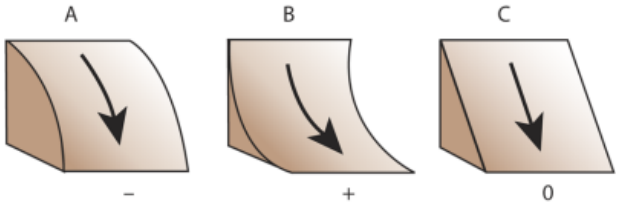

Figure 4.2: Profile curvature is parallel to the slope and indicates the direction of maximum slope. It affects the acceleration and deceleration of flow across the surface (Kimerling et al. 2011).

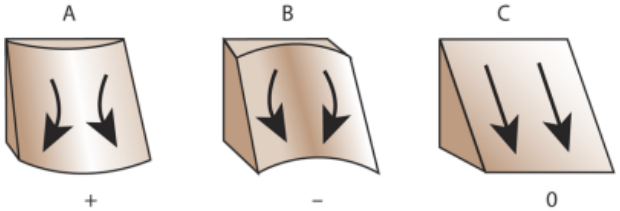

Figure 4.3: Plan curvature is perpendicular to the slope and affects the convergence and divergence of flow across the surface (Kimerling et al. 2011).

Local contrast stretch (LCS) and residual relief separation (RRS)

(Otto & Smith 2013, 5) describe two other common methods which were not used in this study. "LCS (Smith & Clark 2005) uses the concept of relative elevation and that a landform is spatially distinct from neighboring features - a standard linear contrast stretch is applied to a region of a specified size, thereby providing a localized increase in contrast. RRS (Hiller & Smith 2008) takes a different approach and begins with the conceptual understanding that landscapes are comprised of different elevation elements that are 'stacked' on top of one another - these often occur at different width-scales and if the regional-scale relief is removed, then the small-scale 'remainder' (or residual) can be extracted. These residuals ideally only contain features of interest, however as this is a scale-based technique it will contain all features at that scale and this can include anthropogenic features".

Contour and contour slope

Contours or isolines are linear features that all have the same elevation, whereas contour slope shows areas where the slope is identical. Ridges and gullies are well seen with contour lines: for both types of contour lines the level of detail can be defined; for isolines in meters of elevation and for contour slope either in degrees or percent of slope. Since the contours are linear attributes, they can easily be combined with the areal attributes described before.

Combined viewing

Relief shading and curvature can be combined to augment specific geomorphologic features. Therefore the hillshade layer is displayed with a transparency of 20-30% and the wanted curvature layer is placed behind it (proposed workflow from the ArcGIS Resources Blog (Buckley 2010)). The curvature layers, relief shading and an aerial image can be joined in all possible combinations and different transparency rates. Each combination is advantageous to reveal certain features possibly better than by other combination. Therefore one often has to experiment with the different settings to find the optimal solution for the chosen area. The combined views can be extended with a linear contour layer. Looking at all these layers over each other at the same time reveals an overloaded, hard to interpret screen but can give additional information.

4.6 Map visualization and legend generation

The map is designed following the layering system presented by Gustavsson et al. (2006). It consists of the following layers:

- Background image, shaded relief or orthophoto
- Process domain
- Hydrography
- Morphometry
- Morphodynamics, erosion/deposition
- Signatures

Background image

As background the newest shaded relief available is used with an illumination from north-west. It is the same familiar illumination used by the Federal Office of Topography swisstopo despite it being illumination that does not exist in reality (sun stands in the south).

Process domain

The process domains are digitized with the help of all the layers that are described in section 4.5 and following. The coloring is a mixture of all the legends introduced before. Each process has got its own color, mixed ones use the colors of both processes and are displayed in stripes as Jan-Christoph Otto proposes. The colors are the same as IGUL uses and are in similar shades of color that all the other legends use for the processes: *violet* for glacial, *pink* for periglacial, and *green* for fluvial (because *blue* is reserved for the hydrology layer). The gravitational process domain is painted in *orange-brown*. The colors are better distinguishable than those used by Jan-Christoph Otto.

Hydrology

Lakes and running waterways are displayed in blue in the hydrography layer. They are thinner than most other linear features because they are not overly important, but they are a great help in the interpretation of the general setting of the situation displayed on the map. They can clarify the outwash plain.

Morphometry

Contour lines are the most common way of representing slope on a map. They are drawn at an equidistant of 10 m. Every 100 m the contour lines are broader than the prior ones. The lines are highly smoothed and therefore loose some information. They are held in gray.

Morphodynamics (differentiation of erosion and accumulation areas)

Zones with erosion and deposition are displayed in one layer. Starting with the differentiation of two DSM, each cell is classified into *erosion*, *deposition* or *no movement*. The threshold for *no movement* is again the ±20 cm for the periods 2005 to 2009 and 2009 to 2010. For the last period the values -35 cm to 20 cm were used. The area of movement is otherwise to big and does not represent reality. Since a map is a visual representation of reality its generalization helps to show the reader what really happens and to ignore inaccuracies of the data. Next, the single cells are aggregated to smoothed clusters. Very small clusters and those outside of the area of interest are deleted and modified in a second step of generalization towards a readable map.

The outlines of the area are displayed in *red* for erosion and *blue* for deposition. The stroke style defines to which period the outline belongs. For the main geomorphological map only the outlines are used. The interpretation of all these lines, dots and squares are not very easy. Therefore an additional map, only displaying the morphodynamics layer, the shaded relief and the hydrology layer is needed. There the eroded and deposited areas are filled with the same color. The opacity of the filling is 20%, overlapping areas of two or three periods get more intensive in color. This way areas with constant processes can be detected easily.

Signatures

The missing of most signatures is different to most other maps. Only the moraines, rockglaciers and the glacier outlines are shown. The moraines are displayed by a black dotted line with its according year shown at the beginning and end. The glacier outlines are held in black and are also labeled with the corresponding year. Other signatures that would be easily detectable such as flutes or debris flow channels are not being mapped. For one, the mapping of these forms have never been intended (see section 4.2, but also because the map would be too cramped drawing the attention away from the main interest, the morphodynamics.

4.7 Quantification of processes

The quantification over the whole study site offers a large selection of settings. There are two decisions to be made: First, selecting the parameter of the area and secondly choosing what should be done with the glaciers and its different extents. The area used for quantification is the largest one possible merging out of the dataset of 2005, 2009, 2010 clipped with the one of 2014. Concerning the glaciated area the problem of the retreating glacier occurs. When comparing two different years there is an area that has melted since the older measurement. As the glaciated area is left out, there is a band around the margin of the newer glacier extent, that has only got data of one year. Therefore the glacier extent of the older of the two compared years is always used.

Dividing the process of quantification into the three chapters methods, results and discussion is not that easy. Based on the map and the morphometric attributes, areas are selected and afterwards the volume changes are calculated. Already then a first interpretation is made, and based on that the area is re-modified and the whole cycle begins again. Nevertheless the concept is presented in the three chapters (Methods, Results, and Discusion), despite the iterative workflow.

4.7.1 Over the entire study site

A first look at the whole dataset shows the magnitude of movement in the area. The different glacier extents allow several possibilities to compare the oldest with the newest dataset, but only one possibility to look at the oldest two. All possible combinations are calculated to get more information of certain areas.

4.7.2 Control measurement for accuracy

Areas with no volumetric changes demonstrate the precision of the dataset. The area of the side facing north of the right lateral moraine is selected. The field visit confirms that hypothesis that hardly any movement occurs there because the moraine is covered with vegetation that protects the moraine material to a great extent from fluvial erosion. Furthermore the height of a large flat rock of about 5 m^2 is defined in all four datasets. No elevation change should have taken place at that rock. Eventual difference should give a hint towards the accuracy of the measurements.

4.7.3 In the glacio-fluvial area

The glacier is an unknown factor in the system. Material that is following the slope direction may *disappear* in that no data region of the glacier. Also unknown is the factor of the glacier's slow downstream movements, which is influencing the margin of the deglaciated area. Therefore, looking at the area below the glacier eliminates these two uncertainties. The upper margin is the glacier and the lower margin is the end of the outwash plain. Material that is eroded from the ground moraine is expected to be deposited in the plain. The fine material should also remain in that system because of the sedimentation in the flat big outwash plain.

2010 to 2014

Figure 5.4 bottom left, shows a new channel cut through the middle of the ground moraine and deposited material at the beginning of the flat area. Two areas are formed; the first one recognizing the eroded channel and the accumulated fan and the second one expanding the deposition area to the maximum - using the whole flat area.

2009 to 2010

Three different channels are active where the erosion takes place (Figure 5.4 top right). There are two islands in the middle of the ground moraine with hardly any changes and are therefore left out. Is looks like the sedimentation takes place in the whole plain and therefore all of it is used. The upper left part near the glacier is left out. This area undergoes constant changes of lakes forming and being depleted again, combined with a lot of ice. Two snapshots are not enough to describe the area properly. Thats why that area is not taken into consideration for these calculations.

2005 to 2009

The pattern of erosion and deposition is not as clearly visible as in the other two periods. Therefore the maximal area of erosion and deposition is selected (Figure 5.4 top left).

4.7.4 Slide through the lateral moraine

The collapse of the lateral moraine is visually the biggest change throughout the study site. Volumetric changes for this event and its temporal changes are going to be further investigated.

4.7.5 Densely gullied area

According to the paraglacial theory presented in subsection 2.1.3 the reworking of the lateral moraine should be finished and stabilized. Therefore only the volumetric change of the densely gullied area is calculated.

5 Results

5.1 Data 2014

5.1.1 Fieldwork

The dataset of 2014 was obtained on the 4^{th} of August. During the four flights 421 aerial photos were taken to cover an area of 2.88 km^2. The flights have a large overlap leading to a median of 58546 keypoints per image (Figure 5.1). The drone navigates only with the help of a global positioning system (GPS), an inertial measurement unit and a barometric pressure sensor. Since the number of images and the overlap is very high, a high accuracy is expected in the resulting geodata for this small area.

5.1.2 Data processing

The data collected is in the WGS84 (GRS80 ellipsoid), and UTM coordinates. Therefore the coordinates had to be transformed into the Swiss coordinates LV03 as well as a height transformation into the Swiss height system LN02 was necessary in order to compare them with the existing LiDAR data. The coordinate transformation is done in ArcGIS using the *Project Raster* tool. Transforming the dataset into the Swiss height system is much more challenging. The powerful software FME Workbench is the tool recommended by the Federal Office of Topography swisstopo to perform the transformation. Unfortunately, it is only able to transform vector data and can only transform from the Bessel geoid to LN02, but not from the GRS80, the format of the data. The online tool of the Federal Office of Topography swisstopo does not have this restriction, but the file size is limited to 25 MB. To overcome this size limitation a grid was laid over the area and the extracted values were transformed with the online tool REFRAME (Federal Office of Topography swisstopo 2014). The points are interpolated afterwards and used to generate the new heights. As the area is only 2.88 km^2 in size, differences remain minor and vary by maximally 0.042 m from each other.

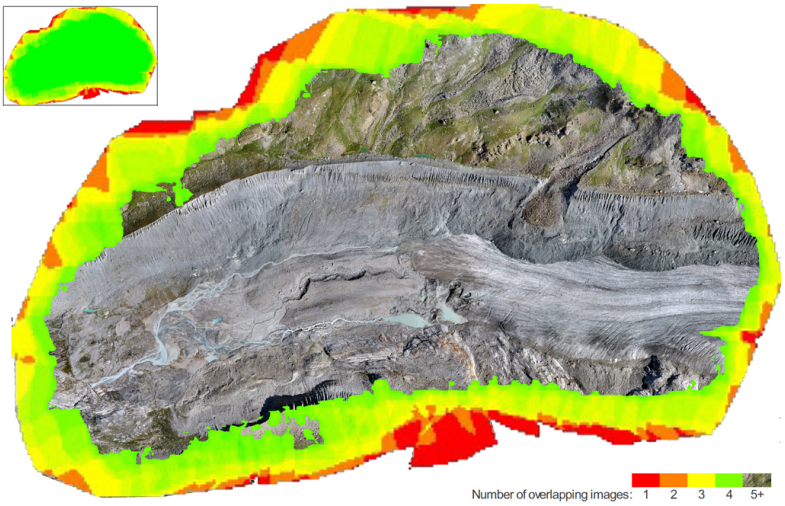

Figure 5.1: Number of overlapping images computed for each pixel of the orthophoto. Red and yellow areas indicate low overlap for which poor results may be generated. Green areas indicate an overlap of 5 images for every pixel. Good quality results will be generated as long as the number of keypoint matches is also sufficient for these areas (out of the Quality Report). The small image shows the original output. The large picture 5+ images is transparent to show where the quality is excellent.

Resampling

The resolution of the 2014 data is 0.118 m. It has to be downsampled to fit the 1 m resolution of the other datasets in order to be comparable.

5.1.3 Accuracy of eBee

The first step towards a co-registration was made to detect horizontal shifts (Nuth & Kääb 2011). The differences showed a pattern that describe the topography, which means one should perform a co-registration. However a few manual attempts could not detect the direction of shifts. The fit due to the extreme high overlapping of often five images or more was much better than expected. Therefore a co-registration was renounced in agreement with Philip Jörg.

5.2 Map

These are the geomorphological and the morphodynamics maps (see Figure 5.2). Larger versions are found in Figure A.2 and Figure A.3.

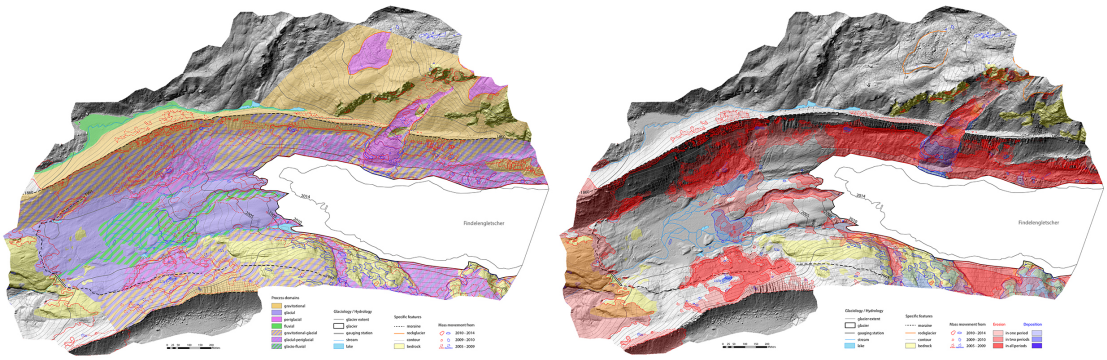

Figure 5.2: Left: the geomorphologic map of the study site. Right: the morphodynamics map. Findelengletscher (VS), Switzerland.

5.3 Quantification of processes

The results are displayed in tables which all have got the same setup. The rows show the period of the calculation and are placed in between the two measured years. The lowest row is an overall calculation of the maximal time period from 2005 - 2014. Not all columns are used in the tables. 'glacier extent' revealing which glacial extent was used for the calculation. 'g10' stands for glacial extent of 2010. Suffixes like *pink* indicates in which color the outline of the area is marked in the corresponding figure. '+dV' and '-dV' refer to the volume is gains and loses in the area, whereas 'dV' is the sum of both figures. To make the areas comparable volume changes are areal adjusted 'dH/A' showing the gains or losses per area. Last the 'annual dH/A' adjusts the height changes to an annual rate and thus is comparable with other areas.

5.3.1 Over the entire study site

Within the entire study site (except the glacier) there is an average loss of -0.12 to -0.32 $\mathrm{m\,a^{-1}}$ per year, depending on the setting of which year and which glacier extent was used (see Table 5.1 **A**).

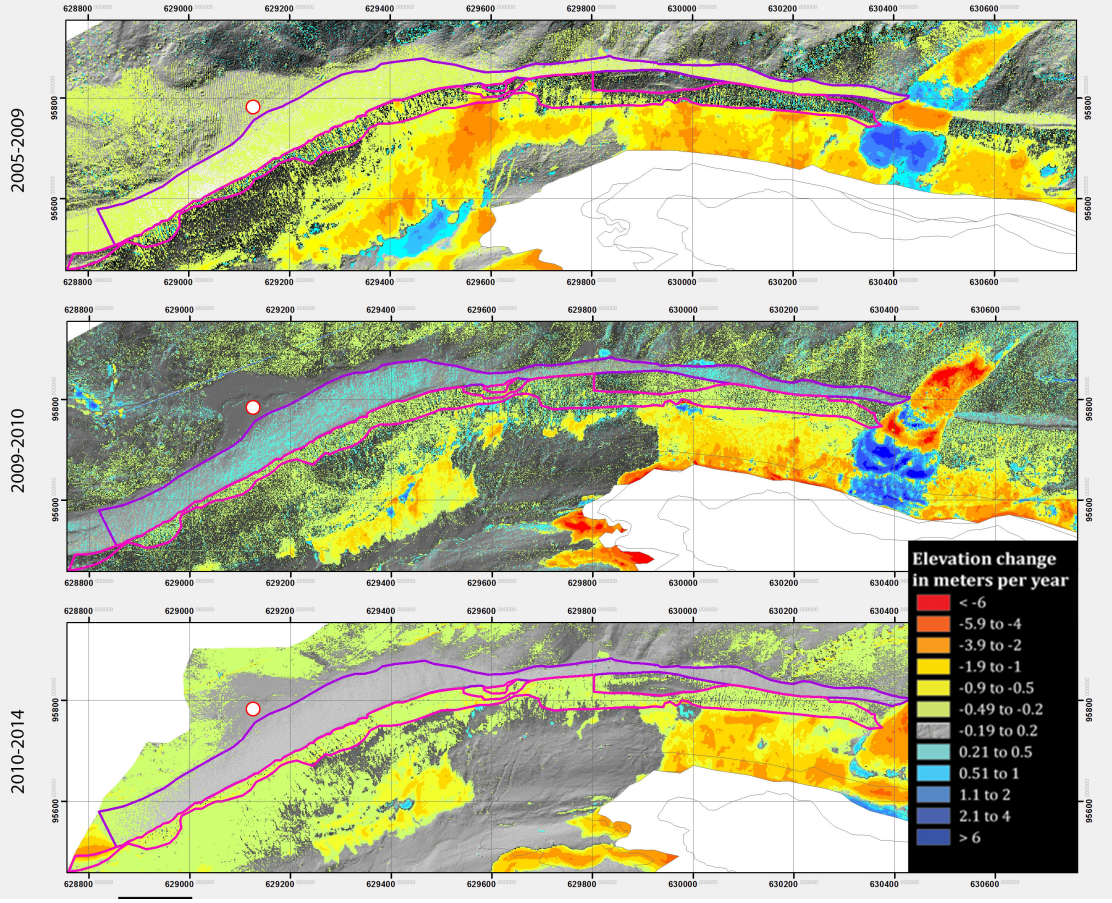

Figure 5.3: Elevation changes in areas defined the control measurements (*violet*) and the gully system (*pink*) used in Table 5.1. The point (*white* point with *red* stroke) indicates the location of the point measurement.

5.3.2 Control measurements for accuracy

The volume change of the area where no shift is expected is very small. From the first to the last measurement each meter of the area loses -0.77 m, or -0.09 ma^{-1} per year (see Table 5.1 **B**). The single point measurement reveals similar sizes with loses of -1.19 m and -0.13 ma^{-1} per year (Table 5.4).

A overall

year	glacier extent	A [m^2]	+dV [m^3]	-dV [m^3]	dV [m^3]	dH/A [m]	annual dH/A [ma^{-1}]
2005							
	g05	2042210	188694	-2074140	-1885446	-0.92	-0.23
2009							
	g05	2042210	99996	-353811	-253815	-0.12	-0.12
	g09	2172286	114711	-520471	-405760	-0.19	-0.19
2010							
	g05	2042210	154987	-2428319	-2273332	-1.11	-0.28
	g09	2172286	175437	-2859738	-2684301	-1.24	-0.31
	g10	2196835	183585	-2962434	-2778849	-1.27	-0.32
2014							
05-14	g05	2042210	88940	-4501532	-4412592	-2.16	-0.24

B control lm

year	A [m^2]	+dV [m^3]	-dV [m^3]	dV [m^3]	dH/A [m]	annual dH/A [ma^{-1}]
	m2					
2005						
	77421	282	-45470	-45188	-0.58	-0.15
2009						
	77421	4986	-711	4275	0.06	0.06
2010						
	77421	3101	-21406	-18305	-0.24	-0.06
2014						
overall	77421	439	-59658	-59219	-0.77	-0.09

Table 5.1: The table shows **A** volume changes of the entire study site and **B** changes in the lateral moraine. For the table **A** different glacier extents that are masked (e.g. g09 means that the glacier outline 2009 was used for both years). +dV add up all fields that have a positive elevation change (deposition), -dV all cells with a negative one (erosion), the sum of the both is the total. Elevation change per area, and annual elevation change per area are shown in the last two columns.

5.3.3 In the outwash plain

For all the three different time periods the volume changes are calculated from the ice margin up to the end of the outwash plain. There is way more material eroded than deposited. The detailed results are presented in the following subsections and always refer to Table 5.2 and Figure 5.4 as do the colors.

2010 to 2014

The channel through the middle part of the ground moraine was formed between 2010 and 2014 during a single event (personal Information from M. Huss, 2015). In a first attempt the area from below the glacier up to the end of the deposited fan is quantified (*pink+violet*) resulting in an average elevation loss of -0.52 ma^{-1}. The volume of eroded sediment is 128460 m^3 that means over four times bigger than the volume of the deposited material which sums up to 30939 m^3.

The second calculation (*pink*) uses the same area as before without the upper zone near the glacier. Compared to the previous run, the volume of eroded material is reduced significantly whereas the amount of deposited material remains constant. The annual elevation change per area is -0.35 ma^{-1}.

The last iteration expands over the area to cover the whole outwash plain (*pink+orange*). The annual elevation change per area is again smaller with -0.29 ma^{-1}.

2009 to 2010

The calculations in the second period reveals a balanced sediment budget. The elevation change over the whole area is -0.02 ma^{-1} and thus much lower than the values of the third period.

2005 to 2009

The annual elevation change per area results with -0.16 ma^{-1}.

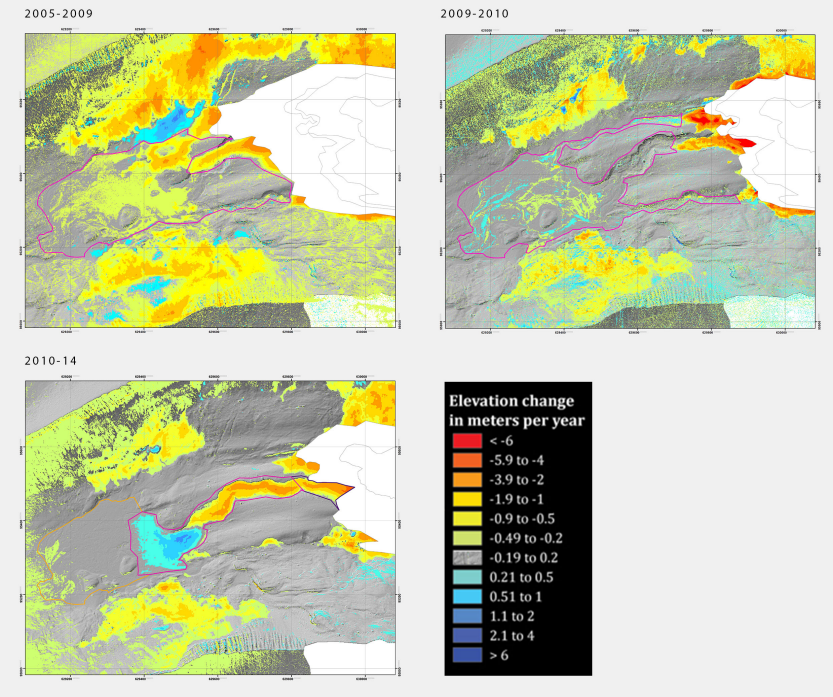

Figure 5.4: Elevation changes used for quantification in areas of glacio-fluvial processes. The colored outlines correspond with the ones in Table 5.2.

fluvial

year	glacier extent	A [m^2]	+dV [m^3]	-dV [m^3]	dV [m^3]	dH/A [m]	annual dH/A [ma^{-1}]
2005							
	g05 $_{pink}$	124722	1251	-80724	-79473	-0.64	-0.16
2009							
	g09 $_{pink}$	109825	2611	-4665	-2054	-0.02	-0.02
2010							
	g10 $_{pink+violet}$	47104	30939	-128460	-97521	-2.07	-0.52
	g10 $_{pink}$	41567	30904	-89439	-58535	-1.41	-0.35
	g10 $_{pink+orange}$	102368	32469	-149782	-117313	-1.15	-0.29
2014							

Table 5.2: Sediment budget in the glacio-fluvial process domain. Different glacier extents that are masked (e.g. g09 means that the glacier outline 2009 was used for both years). +dV add up all fields that have a positive elevation change (deposition), -dV all cells with a negative one (erosion), the sum of the both is the total. Elevation change per area, and annual elevation change per area are shown in the last two columns.

5.3.4 Slide through the moraine

The slide leading to the collapse of the right lateral moraine is visually the first thing seen on a shaded relief or the elevation change visualizations. A compilation of all these maps are displayed in Figure A.7. The area of interest is limited to the area of movement, the sides of the remnant lateral moraines, and the bottom of the glacier extent of 2005. This way the area remains the same over all periods.

In the first period the annual elevation loss is -0.31 m^{-1}. The following periods are all about twice of the foregoing period with -0.82 m^{-1} from 2009 - 2010 and -1.61 m^{-1} for the third period (Table 5.3).

5.3.5 Densely gullied area

The annual elevation change in the gully system area is -0.14 m^{-1} for the first-, -0.16 m^{-1} for second-, and -0.38 m^{-1} for the third period.

A slide

year	glacier extent	A [m^2]	+dV [m^3]	-dV [m^3]	dV [m^3]	dH/A [m]	annual dH/A [ma^{-1}]
2005							
	g05	38237	70513	-118540	-48027	-1.26	-0.31
2009							
	g05	38237	27746	-58985	-31239	-0.82	-0.82
2010							
	g05	38237	1944	-248705	-246761	-6.45	-1.61
2014							
	g05	38237	7566	-333594	-326028	-8.53	-0.95

B gullies

year	A [m^2]	+dV [m^3]	-dV [m^3]	dV [m^3]	dH/A [m]	annual dH/A [ma^{-1}]
2005						
	52555	4631	-34247	-29616	-0.56	-0.14
2009						
	52555	1222	-9364	-8142	-0.16	-0.16
2010						
	52555	80	-80167	-80087	-1.52	-0.38
2014						
	52555	146	-117991	-117845	-2.24	-0.25

Table 5.3: Table **A** shows volume changes of the slide and Table **B** the changes in the gully systems. For the table **A** always the glacier extents of 2005 (g05) was used. +dV add up all fields that have a positive elevation change (deposition), -dV all cells with a negative one (erosion), the sum of both is the total. Elevation change per area, and annual elevation change per area are shown in the last two columns.

control pt		
year	dH/A [m]	annual dH/A [ma^{-1}]
2005		
	-0.64	-0.16
2009		
	0.04	0.04
2010		
	-0.59	-0.15
2014		
14-05	-1.19	-0.13

Table 5.4: Elevation change of a large rock (location: look for the *white* point with *red* stroke in Figure 5.3)

6 Discussion

6.1 Accuracy

Assessing the accuracy of the 2014 data comparing with other existing datasets is hard to estimate. An uncertainty assessment of the LiDAR data was made by Joerg et al. (2012) focusing only on the glaciated area.

For all the datasets an uncertainty of ±20 cm was used. In the images, all values that are smaller than ±20 cm are displayed transparent. Interpreting the images visually, the threshold of 20 cm, selected from the interpretation of the LiDAR data (Joerg et al. 2012), seems plausible. Areas with bedrock, where one does not expect any movement, behave accordingly. The control measurements on the vegetation covered and therefore not supposed to be moving distal side of the northern lateral moraine shows a height loss of -0.77 m in the nine years or a loss of -0.09 m^{-1} per year. The error propagation of the ±20 cm for each dataset can lead to a maximal uncertainty of ±40 cm. It is not very probably that the error reaches the maximal value on average. Therefore the formula from (Nuth & Kääb 2011) is used to estimate the error between two DSMs, thus reducing the error to ±28 cm when using ±20 for both datasets. The longer the timespan, the preciser the results get, because the uncertainty fraction always gets smaller. Due to to the nine year time period, the uncertainties of maximal possible errors are ±4.4 cm and with standard principle of error propagation described by the formula ±3.1 cm. The value of the control measurement of the lateral moraine is, regardless of which of the two values we use, with 9 cm much higher than our estimated error.

$$\epsilon = \sqrt{(imageacuracy\,1)^2 + (imageacurcy\,2)^2}$$

The point measurements show differences in the same magnitude as the control measurements on the moraine. With these assumed *no movement* data the accuracy of all the other calculations can be estimated.

The only question mark lies on the accuracy. Uncertainties are present, can be narrowed down and can be used to put the quantification in perspective. A detailed analysis

on the accuracy of the data would be the next step to give the results even more weight. Therefore a co-registration is inevitable.

6.2 Map

As described in subsection 4.5.1 the interpretation of all the morphometric layers is a demanding task. It is difficult to delimit the zones and assign them to process domains. The process domains do not correlate 100% with the morphodynamic processes found. The borders vary quite a bit, because mass movements are not the only criterion. The interpretation of the surface texture, the orthophoto, and the field site visit for verification are also taken into consideration.

6.2.1 Classification of process domains

Most decisions are obvious when looking at the definition of the process domain (see section 4.3). However some decisions have to be explained. The gully systems are assigned to the gravitational process domain. They are however clearly a part of the moraine, feature of glacial genesis. However the calculations and the interpretation of the exhaustions curves (subsection 6.5.3) show that there is hardly any erosion present in that zone. The remaining processes forming these gullies belong to the gravitational process domain. Analog to this form the backside of the lateral moraine is also assigned to the gravitational process domain. The vegetation protects the slope from wind and precipitation. The erosion is similar to an area without any movement. Consequently they are assigned to the gravitational process domain. The distinction shall highlight zones that are active to the inactive ones yet remains arguable.

6.2.2 Map legend

The legend is similar to those presented in section 2.5. Colors and signatures are all closely related to these examples. The main difference is the new way of visualizing the morphodynamics. Due to the availability of the much preciser data. Four high resolution DSM give the opportunity to define zones of erosion and deposition over the entire study site. The other studies are not able to determine the morphodynamics to such detail and mostly indicate these processes with signatures or large areas in different colors. This resulted in the development of a new method to display the areas of erosion and deposition in their extent as well as their temporal development. Naturally the higher information density leads to a filled map. It can indeed be challenging to determine if

an area is inside or outside a zone. To solve this unsatisfactory fact a second map was created. The filling should reduce the problem described above. By having two maps the morphodynamics layer could have been left out in the geomorphologic map. However, exactly this extra layer adds much additional information to the map. The lines are hard to interpret but do hardly hinder the readability of the other layers. The morphodynamic layer is therefore kept in that map.

6.2.3 Limitations to the methodology

Area behind the moraine of 1991

In all the LiDAR datasets the area below the moraine of 1991 is not in movement. This changed significantly when the 2014 data were included. As can be seen in Figure A.6 there is a large area of erosion. This is not realistic as a big part of that flat area is bedrock or moraine material with flutes and it lies above the fluvial waterway. While creating the morphodynamics map the threshold of erosion had to be increased from -20 cm to -35 cm. This enlargement effected the right lateral moraine correctly and minimizes the expected area when only interpreting the orthophoto and the other morphometric layers. The threshold is however still too small for the area behind the 1991 moraine and still overlaps big areas of bedrock.

Deposition on left lateral moraine

The same error occurred in the area of deposition on the left lateral moraine. The biggest parts of the deposition area are in the zone with bedrock. There is no movement expected there. Also the possibility of material falling down from a steep rock wall can be excluded. There is a rock band above the area, but it is protected by the lateral moraine. The poor coverage of images could possibly be the reason for that error as both areas are at the edge of the study site (see Figure 5.1).

There are two ways to deal with this problem. First, the chosen way in this thesis, showing the limitation of this method. The second possibility would be to correct the map manually so that the map exhibits the erosion in a realistic way. This would be the more precise instrument for a evenhanded map user, but information on how the map was generated would be more complicated.

Geodatabase design

High resolution DSMs are well suited to create geomorphologic and morphodynamics maps. Following the workflow of others who also created geomorphological maps in GIS seemed to be best way. Retrospectively a lot of work and research could have been avoided. Defining the dynamics of all tiny areas when digitizing the process domains does not make any sense. When transforming the raster data to vector data information is lost as one aggregates pixel information to zones. Exactly that detail of information is what distinguishes this work from others. Bigger areas would have sped up the time spent in GIS. A new way of displaying the pixel data had to be developed. The selected visualization works well as the zones of erosion and deposition can be easily detected in spatial and temporal resolution.

6.2.4 Moving (spatial), continuous (temporal) morphodnamics

Most of the morphodynamic erosion and deposition are in movement. The direction of mass movement is mostly facing downwards. The most obvious exception is the debris covered glacier described in section 6.4. On the other hand, the best example is the slide through the lateral moraine. The intensity of the movement is not constant as it was one big slide that now slowly creeps downwards. The direction of the movement is continuously facing in the same direction down the slope.

It is not always that easy to determine what is happening in a zone. A complex example involving two different processes is situated in the zone near the end of the ground moraine in the right lateral moraine (Figure 6.1). The bigger of the two movements is an episodic movement similar to the slide through the lateral moraine further up. A large bit of moraine slides down the moraine and gets deposited below (right *pink* arrow in Figure 6.1 top left). The resulting depression can be seen in all the following shaded relief images. Parallel to that event the slope towards the west is moving continuously downhill over all three time periods. This process of motion is clearly moving (spatial) and continuous (temporal).

6.2.5 Static (spatial), continuous (temporal) morphodynamics

Different to the previous section, there are some areas where changes are static. The biggest one is below the ridge of the left lateral moraine on the height of the outwash plain. The subsided surface hardly shows any changes in all time periods. The areas are getting smaller over time. This strongly suggests that there is a dead-ice block below that spot which is slowly melting away, and consequently lowering the area.

The part on the right lateral moraine below the gullies ranging from the slide towards the end of the glacier behaves similarly. Together with the retreat of the glacier, the zone of erosion is also moving backwards. There are nearly vertical lines along the moraine that are reciding every year. Also the rear part appears to decrease the area from each period to the next. The upper margin below the gullied area is pretty stable, as is the lower edge next to the glacier. But defining if it is part of the ice-cored moraine or a dead-ice block that is melting cannot be said.

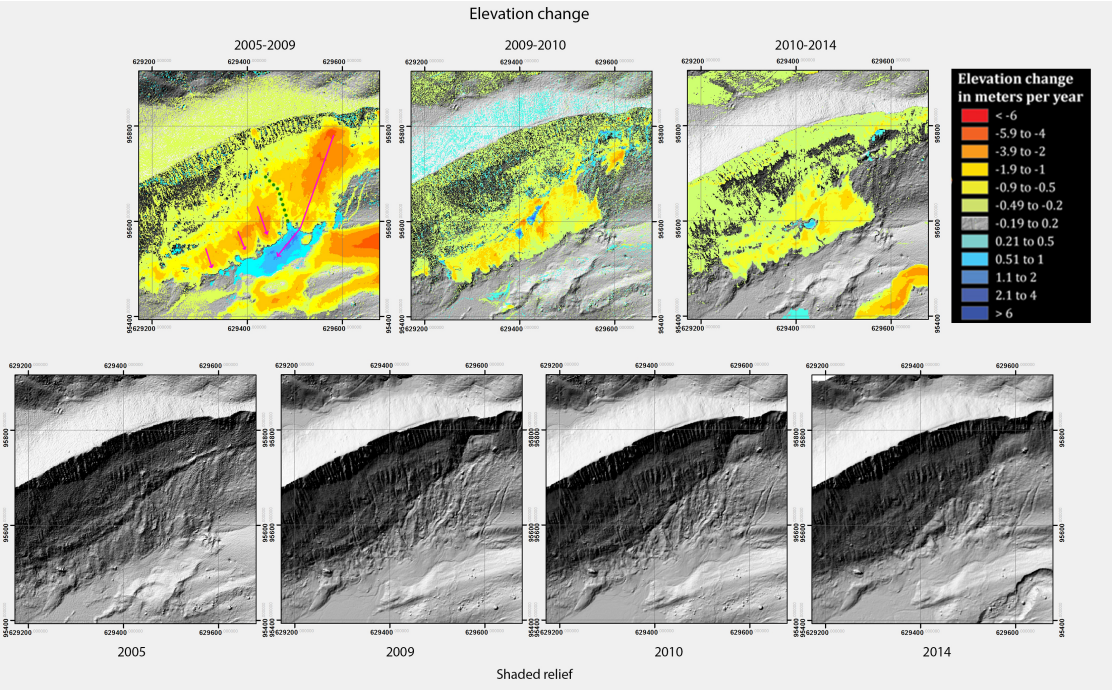

Figure 6.1: The four images at the bottem show shaded reliefs of each year. The elevation changes images are sited between the two corresponding years. In the first period two processes are visible: a big slide on the right side and smaller creeping at the left side (processes are divided by the *green* dotted line). In the following period the big slide stopped and deposited material is reworked by the smaller continuous slide.

6.3 Magnitude of the surface lowering

The area was lowered 2.16 m which is 240 mm a^{-1} in the nine years examined. This is much higher than the denudation rates for highmountain areas (see Table 6.1). For the beneighbored Turtmanntal which does not have a valley glacier, denudation rates range from 0.62 - 1.87 mma^{-1} and for the Hungertälli, a sub-valley where the uncertainties are much smaller than for the entire valley, were calculated to range from 1.42 - 2.64 mma^{-1} (Hinderer et al. 2013).

Location	Denudation rate (mm/a)	Time period	Source
Turtmann Valley (Switzerland)	0·62–1·87	Post-glacial (10 ka)	Otto(2009)
Hungerlitaelli (Switzerland)	1·42–2·64	Post-glacial (10 ka)	Otto(2009)
Walensee (Switzerland)	>1·5	15 ka	Müller (1999)
Upper Rhone Valley (Switzerland)	0·95	Late + post-glacial	Hinderer (2001)
Alps (mean)	0·62	Late + post-glacial	Hinderer (2001)
Bündner Rhine (Switzerland)	0·581	Quaternary	Jäckli (1957)
Langental (Italy)	1·1	Post-glacial	Schrott and Adams (2002)
Reintal (Germany)	0·3	Post-glacial	Hufschmidt (2002)
Alps (mean)	0.32	Present day	Hinderer (2013)
Rhone/Brig (Switzerland)	0·35	Present day	Schlunegger and Hinderer (2003)
Rhone/Port de Scex (Switzerland)	0·15	Present day	Schlunegger and Hinderer (2003)
Vispa/Visp (Switzerland)	0·72	Present day	Schlunegger and Hinderer (2003)

Table 6.1: Denudation rates calculated for entire drainage basins (Otto et al. (2009) modified).

Denudations rates are two orders of magnitude smaller than what is calculated in the study site. There are two possible explanations for tis difference. First, a great amount of sediment leaving the system through the gauging station. In the gauging station there is a big tank which filters the sediment before the water is lead away towards a dammed lake. The tank has to be emptied from time to time, so there might be a way to quantify the amount if the hydropower operators have any data how often the tank is emptied and how full it was. Second, the sacking of the landscape resulting from the melting ice. This is for sure the fact below the glacier tongue (see Figure 5.4). Also some parts of the moraine seem to be ice-cored. The map of the lateral moraine shows that some parts are sliding while others are not stable. The surface texture appears to be finer there and shows that more water is present in these parts of the moraine than in others. In the upper part of the moraine moisture is detected on the same elevation at several spots (Figure 6.2). The level is about 15 m lower than the lakes of the distal side of the moraine. Therefore it is likely to be the margin of the ice-core in the moraine (Kjaer & Kruger 2001). Some lower parts are even wetter, there dead ice is hinted. A visit to the field supports these finding. Near the glacier tongue the ice is visible with only a few centimeters of debris covering it.

As the dimension of denudation rates is known, an about 100 times larger fraction must be accounted to the melting of ice, which leads to the sacking of the landscape.

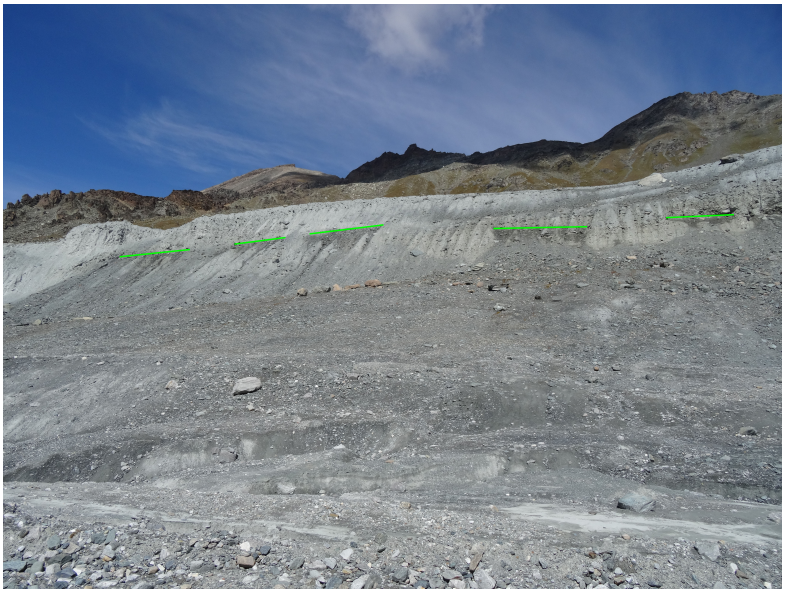

Figure 6.2: The *green* lines indicate wet areas (darker) where water is presumably pressing through the moraine from the river and tiny lakes at the same elevation on the other side of the moraine, at Findelengletscher (VS), Switzerland.

6.4 Glacier extent vs dead-ice

The results of 2010-2014 can be divided into three zones because of the three different glacial extents calculated (see Figure 6.3). The zone closest to the glacier (*red*) with -0.96 m^{-1} and the next one (*orange*) with -0.79 m^{-1} per year have extremely high values compared to the average of the whole area of -0.32 m^{-1}. The zone outside the area of the glacier extent of 2005 (*yellow*), is with -0.28 m^{-1} about three times smaller than the two areas described before. This shows that zones along the glacier margin contain more melting ice leading to increased sacking rates.

Debris covered glacier

In the area along the right glacier margin above the slide an interesting coloring can be discovered. In the second period there is a sequence of elevation loss, gain and so on continuing to move along the flow direction of the glacier (Figure 6.4). The specific pattern occurs when there is a sinuous wave that moves. High areas get lower and lower areas get higher, giving the area that coloring. It clearly shows that this zone is not part of the ice-cored moraine, but is a debris covered part of the glacier. That glacier zone has not been considered in the glacial outlines that were provided for this thesis (see section 3.2.1).

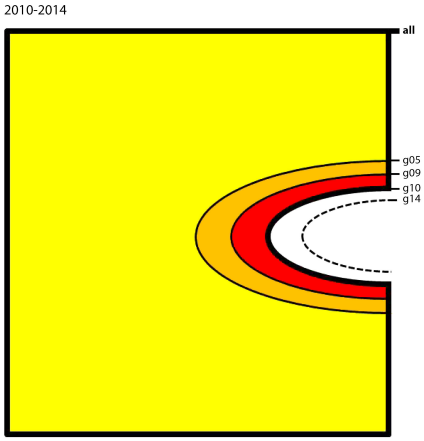

year		A [m^2]	dV [m^3]	dH/A [m]	annual dH/A [ma^{-1}]
2010					
	red	24549	-94548	-3.85	-0.96
	orange	130076	-410969	-3.16	-0.79
	yellow	2042210	-2273332	-1.11	-0.28
	all	2196835	-2778849	-1.26	-0.32
2014					

Figure 6.3: The visualization shows the distribution of annual elevation loss from 2010 to 2014 of the table on the right side. The closer the area is to the Glacier, higher the annual elevation loss is.

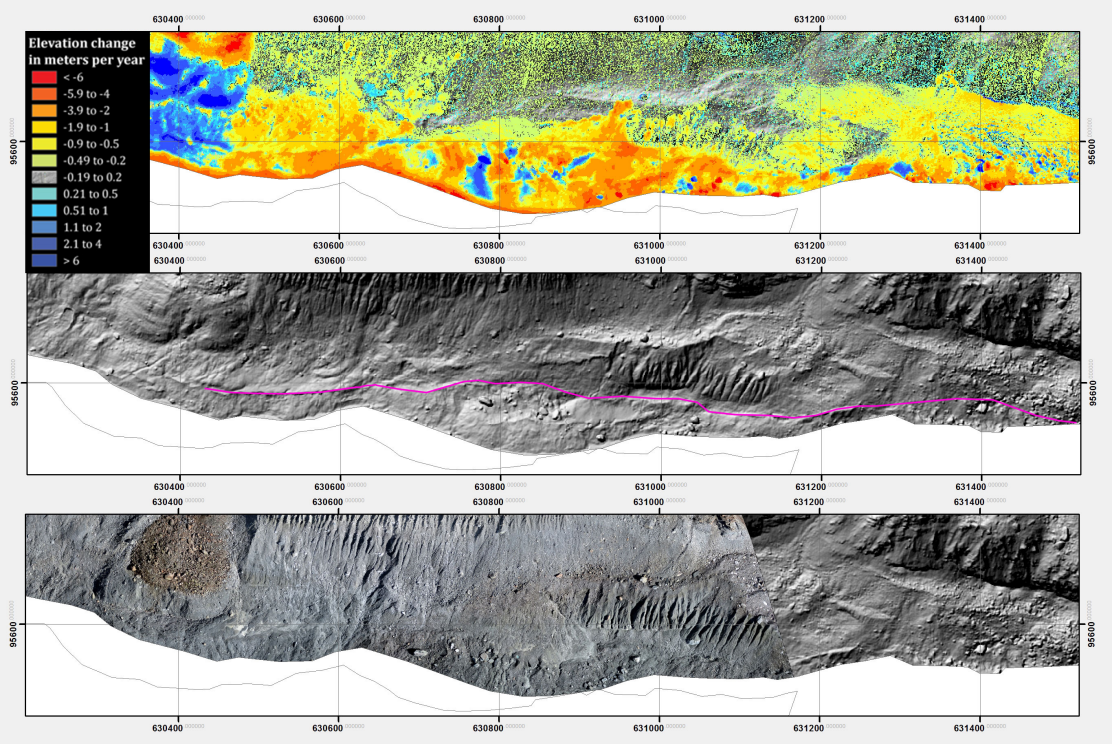

Figure 6.4: Top: Elevation changes from 2009-2010. Middle: Shaded relief from 2010, the pink line indicates the border of the glacier. Bottom: Orthophoto of 2014, areas outside of the 2014 measurement show again the shaded relief of 2010. Some parts of the glacier are debris covered and move in the same direction as the glacier, whilst the rest is moving downwards. The border (in the middle figure *pink* line) can be identified in all images.

6.5 Interpretation of the quantified zones

6.5.1 Glacio-fluvial area

The area remaining below the glacier tongue is in constant change. At the time of the drone flight, the glacial runoff was flowing mainly through the orographic left of the three channels. A month later the lake in that region began draining through the middle channel. Its astonishing that most measurements concerning the area below the glacier show a much larger erosion volume than deposited volume. This phenomena can best be explained by looking at the data of 2010 to 2014.

For the *pink+violet* area as shown in Figure 5.4 four times less material is deposited in the alluvial fan, than is eroded. The material cannot 'disappear' but there are two possibilities. First, the area of erosion is too big. Along the glacier tongue there are areas with ice. The *pink* area cuts off the eroded area that appears to be connected to the glacier rather than to the channel (Figure 5.4 bottom right). The result gets better, but is still unbalanced by a factor of three. One could try to clip an even greater area from the top to balance the result even more. But a field visit showed that the margins of the channel are dry and therefor there is no or hardly any ice in the ground moraine. Also the interpretation of the other periods on the ground moraine show that the area is very stable except for the eroded channels. The second reason might be, that sediments get deposited below the fan. Values ± 20 cm are made transparent, so it could be that over the whole plain the deposition could sum up a whole lot and yet not be visually seen. The *pink+orange* area has got an even larger unbalanced coefficient than both results before. The volume of deposited material stayed similar but the amount of erosion is 67% larger. This is precisely the opposite of what was expected (keep the area of erosion the same size and increase the deposition area to detect more deposition).

The annual elevation changes per area show that he values get lower with each run. The areal reduction from the first to the second calculation seems plausible as the area with ice is left away. For the *pink+orange* area the lowering is only due to the influence of the more than double sized area. Therefore the selection is no improvement to the results of the *pink* area.

The middle channel was eroded in one single event (see section 5.3.3) and is in 2014 approximately 40 m wide and 12 m deep. The dimensions of that channel could give an indication of how much runoff there has to be to form a channel this size in such short time. For sure, very fine material is not being sedimented entirely in the outwash plain and leaves the system. It is however impossible that the whole difference can be accounted to that phenomenon.

In the 2009 - 2010 period the erosion and deposition of new stream ways can be seen in the outwash plain. New channels are made and previous ones are being abandoned (see Figure 5.4 middle image). In the other periods these paintings cannot be found. Probably the reason is that the periods are over four years. The reshaping of one year is reshaped three further seasons and typical forms could be averaged. The ratio of erosion to deposition is with 1.7 by far the lowest. The image as well does not show any large mass movements, and the annual elevation change per area is with -0.02 m way better than the control measurements. For this specific area and time period it seems to be true that sediment get redeposited within the area.

The results from 2005 - 2009 have got an impossible erosion to deposition ratio of 65. There is no plausible argument to be found that could explain the immense dis balance. For sure there must have been some ice that was melting in the area, but the fact that there is no zone of deposition to be found is somewhat staggering. This would mean that most of the eroded sediment managed to overcome the outwash plain and leave the area.

6.5.2 Slide through the lateral moraine

During the first period the moraine collapsed. In the following two periods the whole area continued to slide downwards slowly. Every year the glacier gets pushed back a bit further leaving a good visible dent in the glacier extent of 2014. In the shaded relief of 2005 already appears that some material is blocked by the moraine and the pressure that is built up can be assumed by the convex bulge on the proximal side of the lateral moraine.

In all periods the border between the end of the slide and the compressed zone is visible in all shaded reliefs and elevation subtractions. The zone below that border gets compressed between the slide and the glacier and thus gains height (*blue* coloring along the glacier margin in the second and third period of Figure A.7). The orthophoto (Figure A.1) and older aerial pictures show a differentiation from the grayish moraine material to the *reddish* color of the material above the moraine. A pretty good guess can be made as to where the moraine material is dislocated.

The collapse of the moraine was probably one big event. In the landslide scar it shows that the surface has stabilized by 2009. However below that zone, there is a still an ongoing downhill creep. The bedrock shows that the entire part of the ice-cored moraine (Lukas et al. 2012) was moved away down to the base. The characteristics of the

creeping and the fact of containing frozen material indicates that the collapse conducts like a rockglacier. The resolution of the datasets would allow to trace some big blocks over time. The velocity of the creeping can be determined and compared with other rockglaciers.

The annual elevation loss rates are almost doubling in every period from -0.31 m to -0.82 m and to -1.61 m. Because of the area limited at the bottom always with the glacier extent of 2005, with every year more material is creeping downwards and out of the selected area. As in all other areas, some part of the elevation loss is likely due to ice melting.

6.5.3 Densely gullied area

According to the paraglacial cycle presented in subsection 2.1.1 as well as the interpreting Figure 6.5 show the rapidity of the paraglacial cycle of sediment-mantled slope modification due to the stabilization or exhaustion of metastable sediment sources. Curry et al. (2006) state that the half-live for the formation and stabilization of mature gullies is 15 - 20 years at a total duration of 80 - 140 years in Swiss Alps. The investigated modifications of Glacier du Mont Miné and Feegletscher started $<$64 and $<$88 years ago. Because of the areal proximity Findelengletscher should be in the same timespan as these two glaciers. and the available sediment remaining of 0 - 12% must be similar (Figure 6.5). The calculations support that theory. There is still some sediment left as the annual average elevation loss is slightly larger than the control measurements (see Table 6.2). The gullies are not vegetated which also indicates that the modification has not yet finished.

Compairing the calculations, the biggest difference results yet again from the last period. There is an overestimation, analog to the problems of the dataset described when creating the morphodynamics map layer.

	gully	control lm	control pt
year	annual dH/A $[ma^{-1}]$	annual dH/A $[ma^{-1}]$	annual dH/A $[ma^{-1}]$
2005			
	-0.14	-0.15	-0.16
2009			
	-0.16	0.06	0.04
2010			
	-0.38	-0.06	-0.15
2014			
	-0.25	-0.09	-0.13

Table 6.2: Elevation changes in gullied area, compared to areas with no movement. In the first period the rates are nearly identical whereas in the second and third period the differences are clear. The gully system is still being reworked and has not yet stabilized.

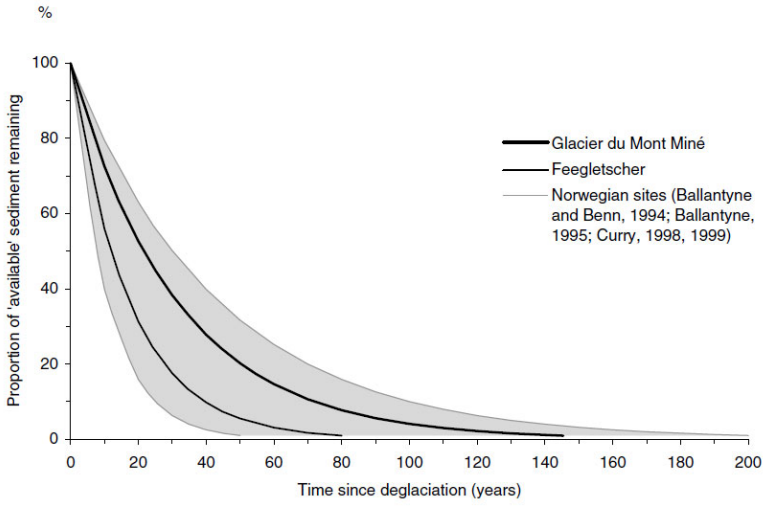

Figure 6.5: Exhaustion curves and envelope for paraglacial gully development and accumulation of small debris cones, based on Ballantyne (2002*a*) model and data in this and Norwegian studies (Curry et al. 2006).

7 Conclusion

In the last chapter the research objectives are evaluated. They summarize how these subtasks could be fulfilled and the outlook shows the potential of further research to this topic and study site.

Expand the time series from five to nine years by a drone flight over the study site

The results of the 2014 dataset are promising. The effort of acquiring the data and the processing of the data was very small compared to that of the LiDAR data. For such a small area as the study site is the drone seems the optimal tool to be used. Finding the ongoing processes and quantifying them is well possible.

Create a geomorphologic map showing the morphodynamics

The creation of a geomorphologic and morphodynamics map based on high resolution DSMs is a demanding task. A new way to visualize raster data had to be developed to represent the morphodynamics more accurately.

Distinguish stable areas from areas that are in movement

The map together with the morphometric layers enabled to identify stable areas form areas in movement.

Find out which processes are active and where

The temporal aspects of dynamic areas show the evolution of the processes. The map displays all these developments in an appealing way and helps to describe and interpret the found spatio-temporal movements.

Quantify the sediment transfer budget for the active zones

The quantification shows great results and gives evidence of the findings of the map and the morphography. The magnitude of the movement, over the entire study site, is two

magnitudes bigger than the denudation rates. This results to melting processes that vary greatly depending on which process is looked at.

Outlook

Measuring campaigns are on the Findelengletscher conducted every spring and fall. Since there are now four high resolution datasets of the glacier forefield and glacier tongue area available it could be of interest to let the drone fly over the same area every one or two years. The additional effort would be moderate as the University of Zurich possesses a drone. Including the dataset of 2014 to the Findel-Wiki might be a smart move and thus granting the scientists easier access to the data.

A co-registration should be made in order to determine the error of the 2014 dataset with the datasets of 2005, 2009, and 2010 more precisely.

Creating a map in GIS using many different layers and then just print them is a waste. Using a web map service (WMS) would be the future way. That way a map reader could choose the information of interest and select the relevant layers himself.

The data offers sheer endless possibilities to investigate specific areas and features e.g. to link sediment transfer with the data from the gauging station. Therefore a lot of further research is possible and the area of the Findelengletscher will remain a hotspot for scientists.

A Appendix

A.1 Orthophoto

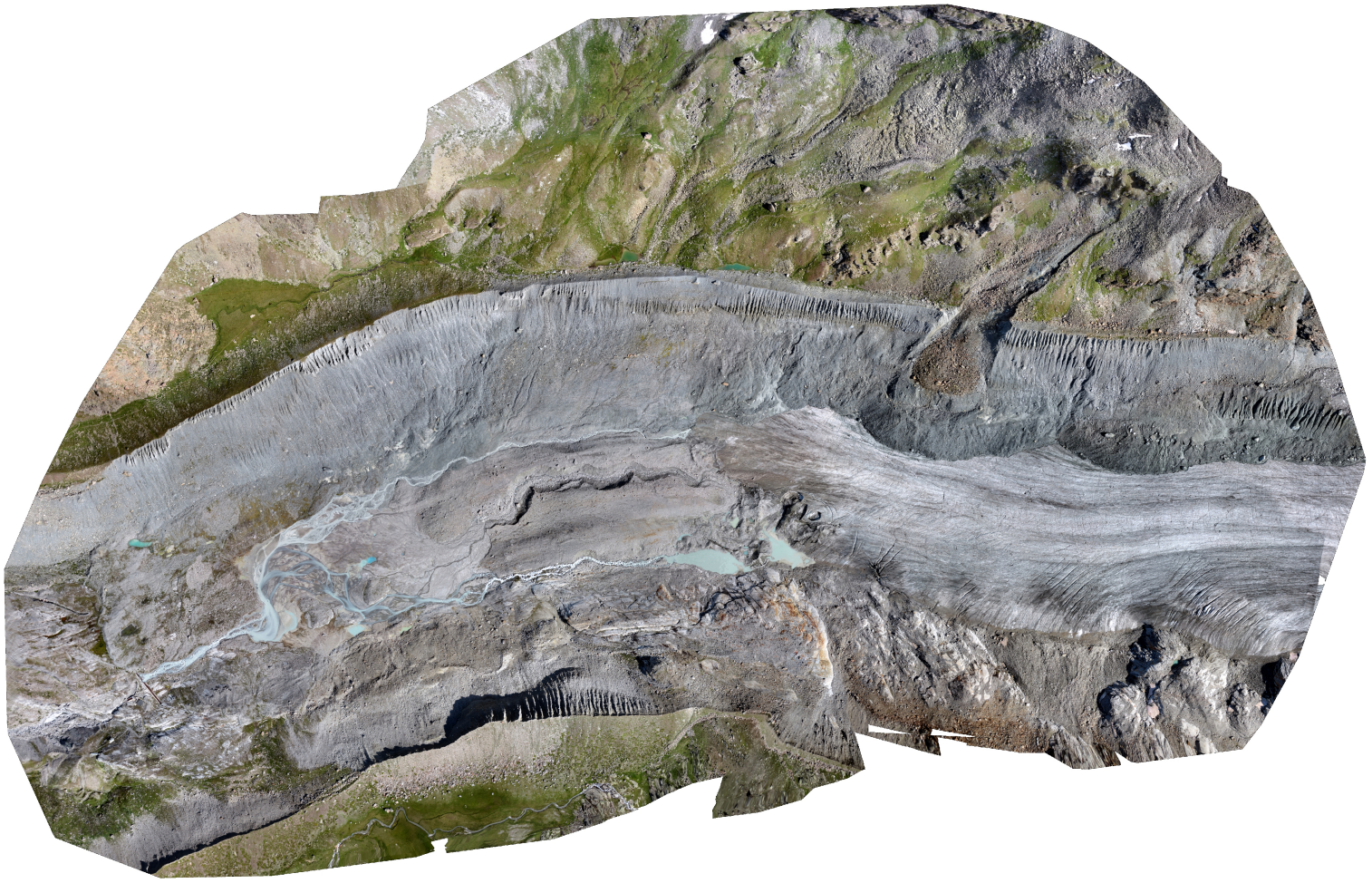

Figure A.1

A.2 Geomorphologic map

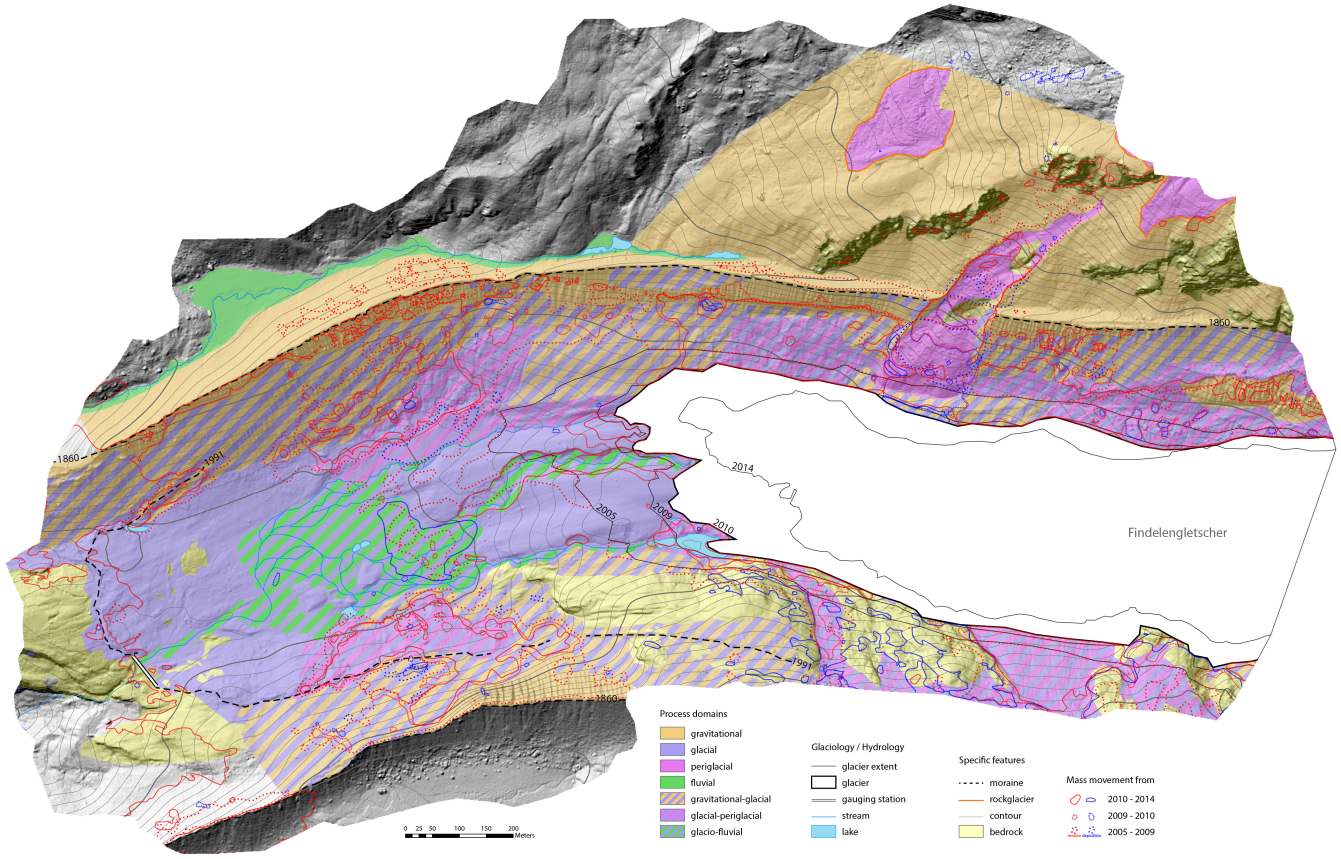

Figure A.2

A.3 Morphodynamics map

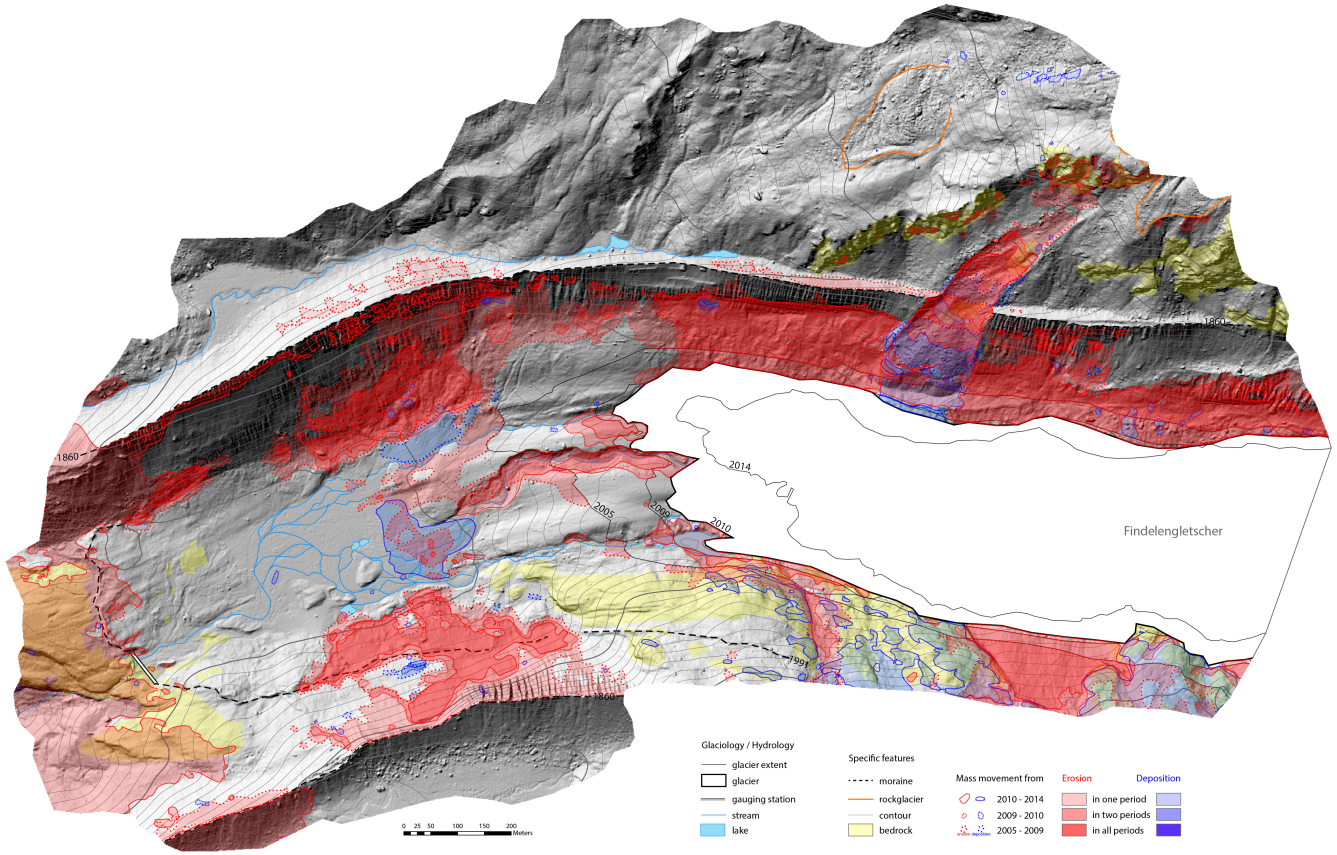

Figure A.3

A.4 Elevation changes from 2005 to 2009

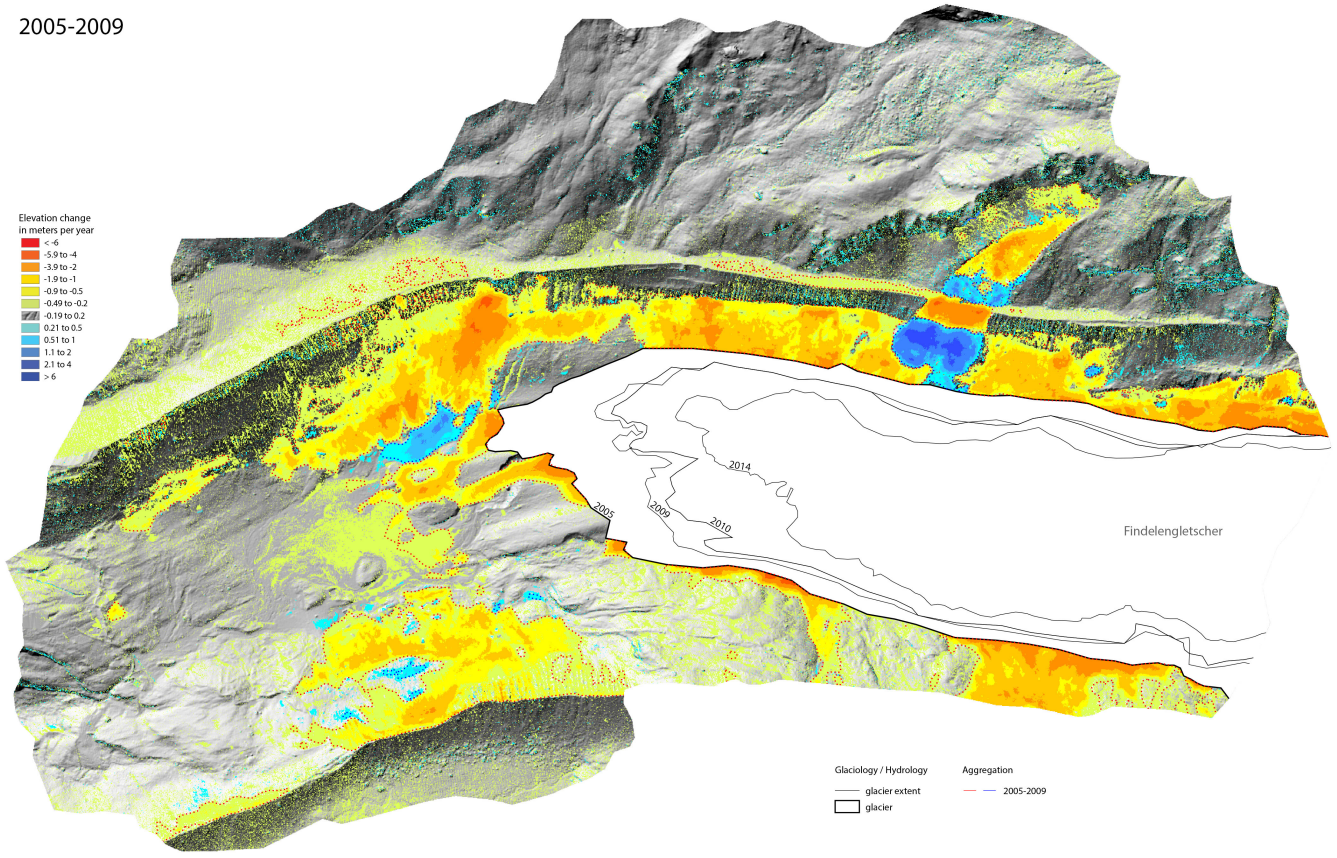

Figure A.4

A.5 Elevation changes from 2009 to 2010

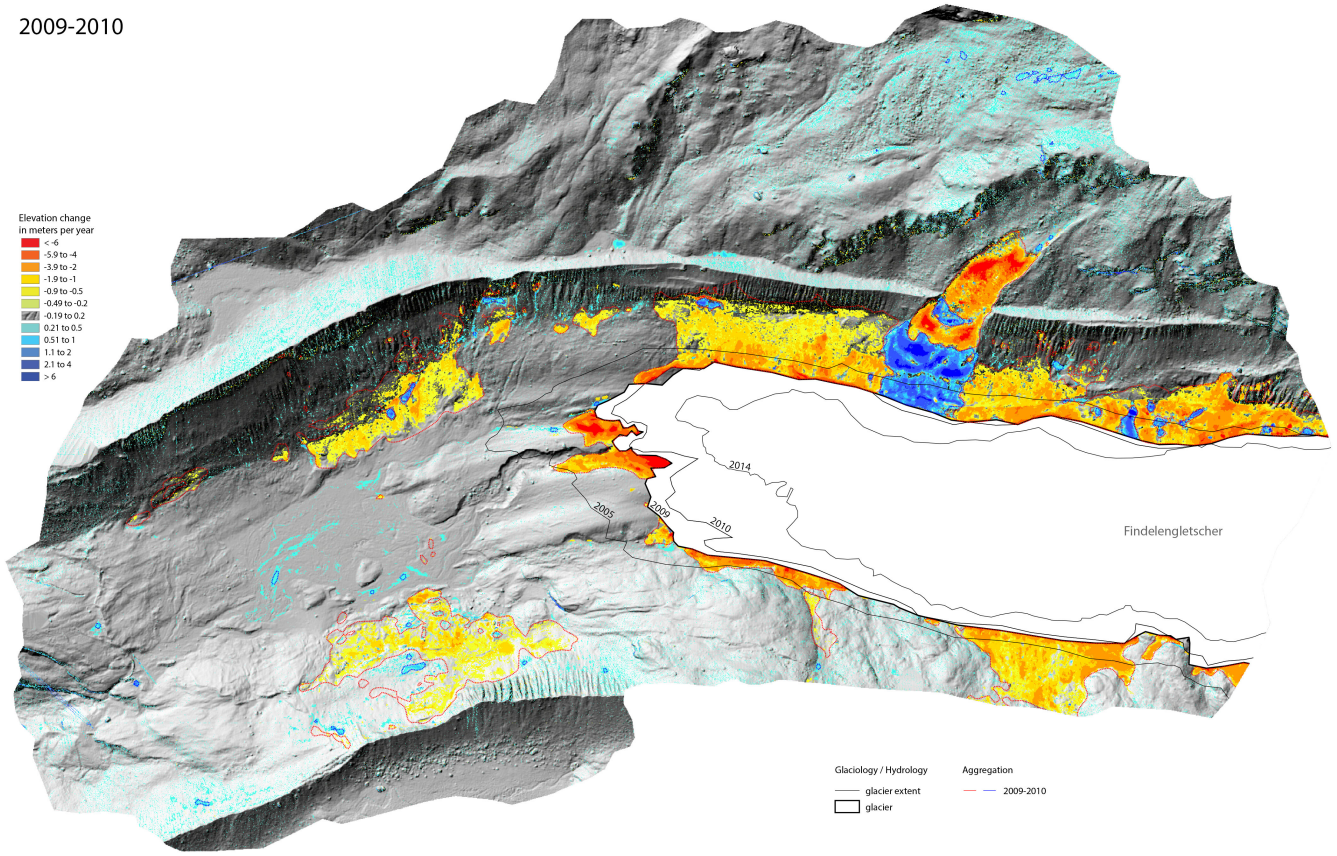

Figure A.5

A.6 Elevation changes from 2010 to 2014

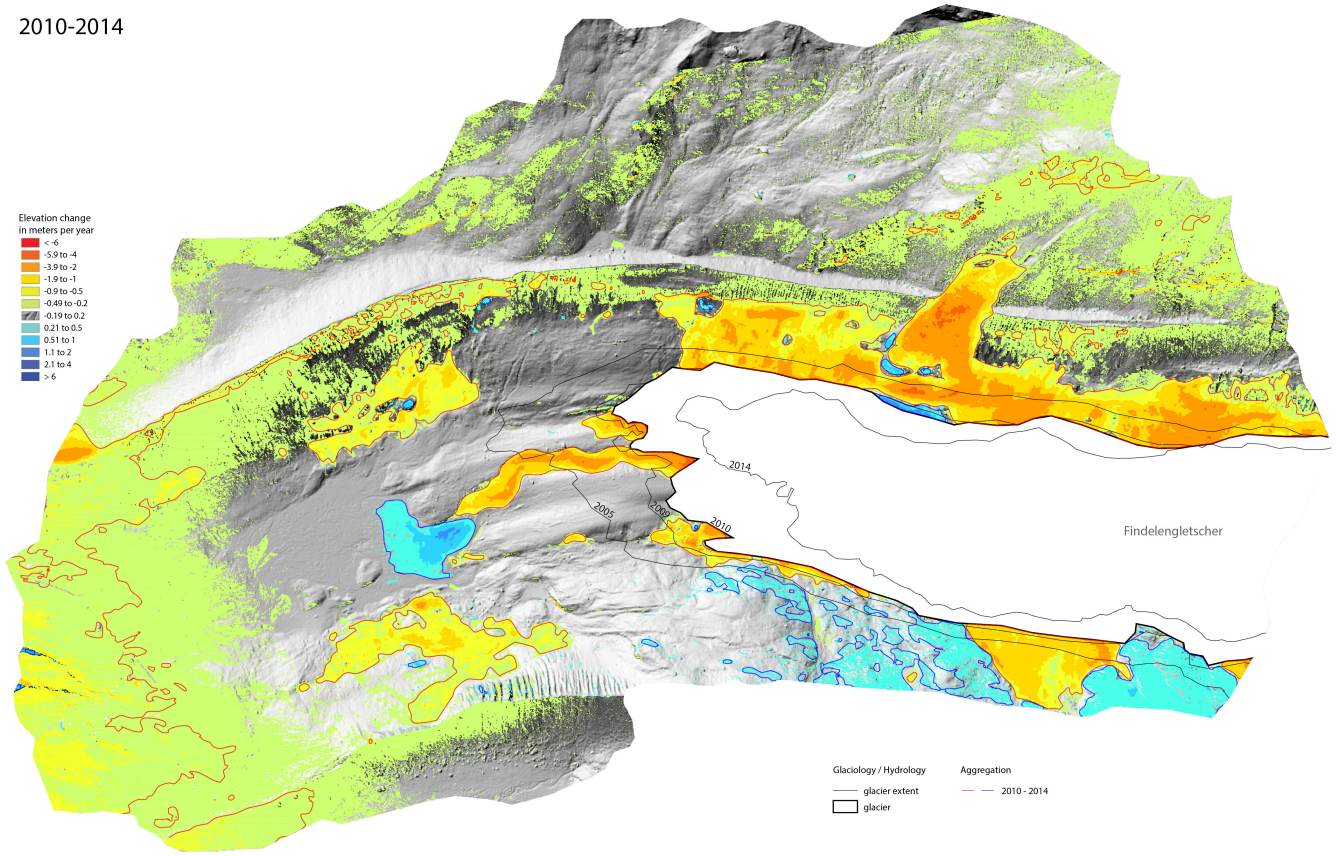

Figure A.6

A.7 Compilation of figures displaying the slide

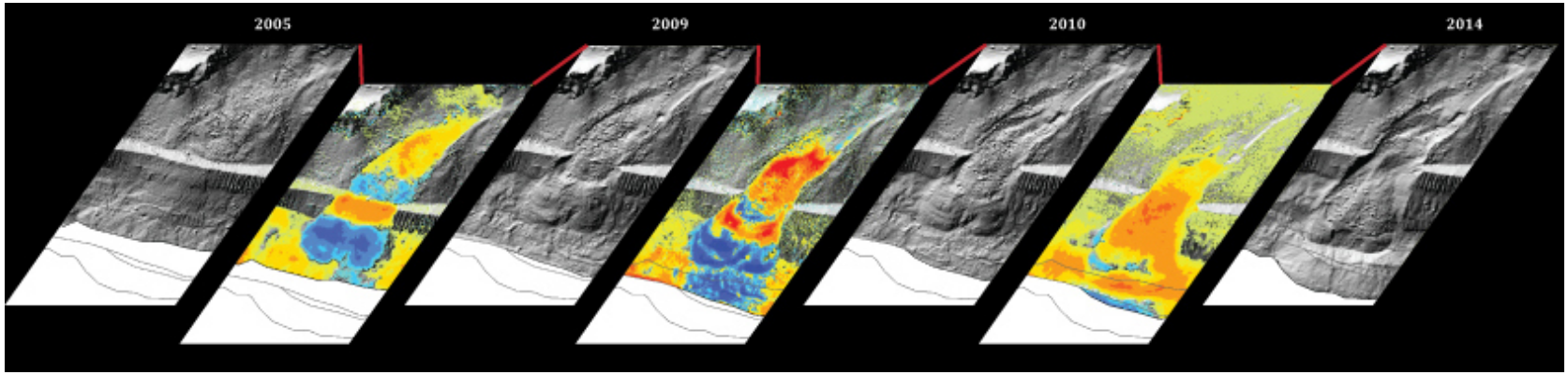

Figure A.7

Bibliography

Ballantyne, C. K. (2002*a*), 'A general model of paraglacial landscape response', *The Holocene* **12**, 371–376.

Ballantyne, C. K. (2002*b*), 'Paraglacial geomorphology', *Quaternary Science Reviews* **21**(18-19), 1935–2017.

Ballantyne, C. K. & Benn, D. I. (1994), 'Paraglacial slope adjustment and resedimentation following recent glacier retreat, Fåbergstølsdalen, Norway', *Arctic and Alpine Research1* **26**(3), 255–269.

Barsch, D. & Liedtke, H. (1980), 'Principles, scientific value and practical applicability of the geomorphological map of the Federal Republic of Germany at the scale of 1:25,000 (GMK 25) and 1:100,000 (GMK 100)', *Zeitschrift für Geomorphologie N.F., Suppl* **36**, 296–313.

Beer, A. (2005), GIS-basierte geomorphologische Kartierung in der Val Chamuera sowie morphochronologische Untersuchungen am Schwemm-/Murkegel der Val Champagna im Oberengadin (GR), Master thesis, University of Zurich.

Bertin, J. (1983), *Semiology of graphics: Diagrams, networks, maps (WJ Berg, Trans.)*, The University of Wisconsin Press, Ltd, Madison, WI.

Blair, R. W. (1994), 'Moraine and valley wall collapse due to rapid deglaciation in Mount Cook National Park, New Zealand', *Mountain Research and Development* **14**(4), 347–358.

Bossard, T. (2014), Evaluation of swissALTI 3D with airborne laser scanning data for applications in glaciology, Master thesis, University of Zurich.

Brardinoni, F. & Hassan, M. A. (2006), 'Glacial erosion, evolution of river long profiles, and the organization of process domains in mountain drainage basins of coastal British Columbia', *Journal of Geophysical Research* **111**, 1–12.

Brun, L. (2012), Analysis of the NCEP / NCAR reanalysis dataset and of cold waves and drought events in Cusco and Apurimac (Peru), Master thesis, University of Zurich.

Büchel, J. (2011), Massenbilanzmessungen am Findelengletscher, Master thesis, University of Zurich.

Buckley, A. R. (2010), 'Using curvature rasters to enhance terrain reresentation'.
URL: *http://blogs.esri.com/esri/arcgis/2010/10/27/using-curvature-rasters-to-enhance-terrain-representation/* (Access: 09.09.2014).

Church, M. & Ryder, J. (1972), 'Paraglacial sedimentation: a consideration of fluvial processes conditioned by glaciation', *Geological Society of America Bulletin* **83**(10), 3059–3072.

Curry, A. M. (2000), 'Observations on the distribution of paraglacial reworking of glacigenic drift in western Norway', *Norsk Geografisk Tidsskrift* **54**(4), 139–147.

Curry, A. M., Cleasby, V. & Zukowskyj, P. (2006), 'Paraglacial response of steep, sediment-mantled slopes to post-'Little Ice Age' glacier recession in the central Swiss Alps', *Journal of Quaternary Science* **21**(3), 211–225.

Demel, W. & Hauenstein, P. (2005), 'Cartography of habitats by Colour Infrared Aerial Images. Guidelines for Delimitation and Interpretation'.
URL: *http://www.parcs.ch/wpz/pdf_public/2013/13175_20131015_145325_HIK-2_2_2_Guidelines_German_Build_001.pdf* (Access: 11.11.2014).

Federal Office of Topography swisstopo (2014), 'REFRAME'.
URL: *http://www.swisstopo.admin.ch/internet/swisstopo/en/home/apps/calc/reframe.html* (Access: 13.08.2014).

Felber, L. (2011), Geomorphologie und Paläoglaziologie im Gebiet Val Tasna/ Val Urschai (GR) und aktuelle archäologiesche Funde, Master thesis, University of Zurich.

Gustavsson, M. & Kolstrup, E. (2009), 'New geomorphological mapping system used at different scales in a Swedish glaciated area', *Geomorphology* **110**(1-2), 37–44.

Gustavsson, M., Kolstrup, E. & Seijmonsbergen, A. C. (2006), 'A new symbol-and-GIS based detailed geomorphological mapping system: Renewal of a scientific discipline for understanding landscape development', *Geomorphology* **77**(1-2), 90–111.

Gustavsson, M., Seijmonsbergen, A. C. & Kolstrup, E. (2008), 'Structure and contents of a new geomorphological GIS database linked to a geomorphological map - With an example from Liden, central Sweden', *Geomorphology* **95**(3-4), 335–349.

Haeberli, W. & Beniston, M. (1998), 'Climate change and its impacts on glaciers and permafrost in the Alps', *Ambio* 258–265.

Haeberling, C. (2000), 'A digital cartographic workflow for glaciomorphological map series - evaluating Macromedia FreeHand as educational tool', *Computers & Geosciences* **26**(1), 29–35.

Hengl, H. I. & Reuter, T. (2009), *Geomorphometry : Concepts, Software, Applications*, Vol. vol. 33, 33 edn, Elsevier, Amsterdam.

Hiller, J. & Smith, M. (2008), 'Residual relief separation: digital elevation model enhancement for geomorphological mapping', *Earth Surface Processes and Landforms2* **33**(14), 2266–2276.

Hinderer, M., Kastowski, M., Kamelger, A., Bartolini, C. & Schlunegger, F. (2013), 'River loads and modern denudation of the Alps — A review', *Earth-Science Reviews* **118**, 11–44.

Huss, M., Zemp, M., Joerg, P. C. & Salzmann, N. (2014), 'High uncertainty in 21st century runoff projections from glacierized basins', *Journal of Hydrology* **510**, 35–48.

Iken, A. & Bindschadler, R. A. (1986), 'Combined measurements of subglacial water pressure and surface velocity of Findelengletscher, Switzerland: conclusions about drainage system and sliding mechanism', *Journal of Glaciology* **32**(110), 101–119.

Imbaumgarten, T. (2005), Kartierung und GIS-basierte Darstellung der Geomorphologie im Gebiet Val Bever / Val Saluver (GR) sowie Modellierung spät- und postglazialer Gletscherstände in der Val Muragl (GR), Master thesis, University of Zurich.

Joerg, P. C., Morsdorf, F. & Zemp, M. (2012), 'Uncertainty assessment of multi-temporal airborne laser scanning data : A case study on an Alpine glacier', *Remote Sensing Environment* **127**, 118–129.

Joerg, P. C. & Zemp, M. (2014), 'Evaluating Volumetric Glacier Change Methods Using Airborne Laser Scanning Data', *Geografiska Annaler: Series A, Physical Geography* **96**, 135–145.

Kääb, A. (2005), 'Remote Sensing of Mountain Glaciers and Permafrost Creep', *Schriftenreihe Physische Geographie* **48**, 266.

Kimerling, A. J., Buckley, A. R. & Muehrcke, P. C. (2011), *Map Use: Reading, Analysis, Interpretation*, seventh ed edn, ESRI, Incorporated.

Kjaer, K. H. & Kruger, J. (2001), 'The final phase of dead-ice moraine development: processes and sediment architecture, Kotlujokull, Iceland', *Sedimentology* **48**(5), 935–952.

Kneisel, C., Lehmkuhl, F., Winkler, S., Tressel, E. & Schröder, H., eds (1998), *Legende für geomorphologische Kartierungen in Hochgebirgen (GMK Hochgebirge)*, Trier.

Koch, R. (2003), Geomorphologische Kartierung im Berninagebeit sowie GIS-basierte Darstellung und Analyse der Geomorphologie im Gebiet Oberengadin (GR), Master thesis, University of Zurich.

Lambiel, C., Maillard, B., Regamey, B., Martin, S., Kummert, M., Schoeneich, P., Pellitero Ondicol, R. & Reynard, E. (2013), 'Adaptation of the geomorphological mapping system of the University of Lausanne for ArcGIS'.
URL: *www.unil.ch/igul/files/live/sites/igul/files/shared/recherche/Geomorphological_legend/Poster_IAG_Paris_2013.pdf* (Access: 14.01.2015).

Leser, H. (2003), *Geomorphologie*, Westermann Schulbuchverlag GmbH, Das Geographische Seminar, Braunschweig.

Lukas, S., Graf, A., Coray, S. & Schlüchter, C. (2012), 'Genesis, stability and preservation potential of large lateral moraines of Alpine valley glaciers - towards a unifying theory based on Findelengletscher, Switzerland', *Quaternary Science Reviews* **38**, 27–48.

Machguth, H., Eisen, O., Paul, F. & Hoelzle, M. (2006), 'Strong spatial variability of snow accumulation observed with helicopter-borne GPR on two adjacent Alpine glaciers', *Geophysical Research Letters* **33**, L13503.

Madella, A. (2013), Analysis of flute-forming conditions in Alpine setting: glacial bedforms at Findelengletscher, Zermatt, Switzerland, Master thesis, University of Bern.

Maillard, B., Lambiel, C., Martin, S., Ondicol, P., Reynard, E. & Schoeneich, P. (2009), 'The ArcGIS version of the geomorphological mapping legend of the University of Lausanne', *Department of Geography, University of Lausanne* .

Maisch, M., Wipf, A., Denneler, B., Battaglia, J. & Benz, C. (2000), Die Gletscher der Schweizer Alpen, 2 edn, Vol. 4, vdf Hochschulverlag AG an der ETH Zürich, Zurich, chapter Gletscherh.

Nuth, C. & Kääb, A. (2011), 'Co-registration and bias corrections of satellite elevation data sets for quantifying glacier thickness change'.

Otto, J.-C. & Dikau, R. (2004), 'Geomorphologic system analysis of a high mountain valley in the Swiss Alps', *Zeitschrift für Geomorphologie* **48**(3), 323–341.

Otto, J.-C., Schrott, L., Jaboyedoff, M. & Dikau, R. (2009), 'Quantifying sediment storage in a high alpine valley (Turtmanntal, Switzerland)', *Earth Surface Processes and Landforms* **34**(13), 1726–1742.

Otto, J.-C. & Smith, M. J. (2013), Geomorphological mapping, *in* L. Clarke, ed., 'Geomorphological Techniques', online edi edn, Vol. 6, British Society for Geomorphology, London, chapter 2, 1–10.

Owen, L. A. (1994), Glacial and non-glacial diamiction in the Karakoram Mountains and Western Himalayas, *in* W. P. Warren & D. Croot, eds, 'Formation and Deformation of Glacial Deposits', Balkema: Rotterdam, 9–28.

Paul, F., Machguth, H., Hoelzle, M., Salzmann, N. & Haeberli, W. (2008), Alpinewide distributed glacier mass balance modeling: a tool for assessing future glacier change?, *in* B. Orlove, E. Wiegandt & B. Luckman, eds, 'Darkening Peaks: Glacier Retreat, Science, and Society', University of California Press, Berkeley and Los Angeles, 111–125.

Pike, R., Evans, I. & Hengl, T. (2009), *Geomorphometry - Concepts, Software, Applications*, Vol. 33 of *Developments in Soil Science*, Elsevier.

Richardson, S. D. & Reynolds, J. M. (2000), Degradation of ice-cored moraine dams: implications for hazard development, *in* 'Debris-covered glaciers : proceedings of an international workshop held at University of Washington in Seattle, Washington, USA', number 264, Wallingford: IAHS Press, 187 – 197.

Rickenmann, D. & Zimmermann, M. (1993), 'The 1987 debris flows in Switzerland: documentation and alalysis', *Geomorphology1* **8**(2), 175–189.

Schmidt, J., Evans, I. S. & Brinkmann, J. (2003), 'Comparison of polynomial models for land surface curvature calculation', *International Journal of Geographical Information Science* **17**(8), 797–814.

Sigurdsson, O. & Williams, R. S. J. (1991), 'Rockslides on the Terminus of "Jökulsárgilsjökull", Southern Iceland', *Geografiska Annaler. Series A, Physical Geography* **73**(3), 129–140.

Small, R. J. (1983), 'Lateral moraines of Glacier de Tsidjiore Nouve: form, development and implications', *Journal of Glaciology* **29**(102), 250–259.

Smith, M. J. & Clark, C. D. (2005), 'Methods for the visualization of digital elevation models for landform mapping', *Earth Surface Processes and Landforms* **30**(7), 885–900.

Smith, M. J. & Wise, S. M. (2007), 'Problems of bias in mapping linear landforms from satellite imagery', *International Journal of Applied Earth Observation and Geoinformation* **9**(1), 65–78.

Sold, L., Huss, M., Hoelzle, M., Andereggen, H., Joerg, P. C. & Zemp, M. (2013), 'Methodological approaches to infer end-of-winter snow distribution on alpine glaciers', *Journal of Glaciology* **59**(218), 1047–1059.

Uhlmann, B., Jordan, F. & Beniston, M. (2013), 'Modelling runoff in a Swiss glacierized catchment-part I: methodology and application in the Findelen basin under a long-lasting stable climate', *International Journal of Climatology* **33**(5), 1293–1300.

Zimmermann, M. & Haeberli, W. (1993), 'Climatic change and debris flow activity in high-mountain areas - a case study in the Swiss Alps', *Catena Supplement* **22**(59-72).

Zuan, M. (2008), GIS-basierte geomorphologische Kartierung im Sihlwald mittels hochau ösendem Laserscan-Geländemodell Marco Zuan, Master thesis, University of Zurich.

Personal declaration

I hereby declare that the submitted thesis is the result of my own, independent work. All external sources are explicitly acknowledged in the thesis

Date & Place: ..... Signature: .....